THE UNIVERSITY OF OKLAHOMA

GRADUATE COLLEGE

THE EFFECT OF REGENERATION TEMPERATURE AND PRESSURE ON THE ADSORPTIVE CAPACITY OF SILICA GEL IN A HYDROCARBON ENVIRONMENT

A DISSERTATION

SUBMITTED TO THE GRADUATE FACULTY

in partial fulfillment of the requirements for the

degree of

DOCTOR OF PHILOSOPHY

BY

ABDEL-KADER M. KOTB

Norman, Oklahoma

1965

THE EFFECT OF REGENERATION TEMPERATURE AND PRESSURE ON THE ADSORPTIVE CAPACITY OF SILICA GEL IN A HYDROCARBON ENVIRONMENT

BY

J. L. Campbell

Charles J. Martin

Arthur Bernhart

DISSERTATION COMMITTEE

ABSTRACT

This thesis represents a pioneer study on the possible role of changes in silica gel characteristics on its adsorptive capacity. It was hypothesized that the elevated pressure and temperature commonly used in regeneration of the gel in commercial processes might consequently alter the structure.

It has been shown for the first time in a semi-quantitative way, that the adsorptive capacity is a function of the pressure and temperature of regeneration. It has further been found that the time of such exposure, i.e., the number of cycles has also affected the adsorptive capacity of silica gel by changing its surface area due to a change in regeneration pressure.

Also the adsorptive capacity of silica gel has been found to be a function of surface area and pore volume. It would appear that any combination of time and pressure that caused a given reduction in surface area would yield a given capacity for the material studied and that pore volume and surface area are dependent variables. Either may be used to characterize gel behavior with pressure and time.

X-ray diffraction was used to investigate the quantitative reasons that affect the adsorptive capacity of silica gel. Three different types of investigations were performed on silica gel.

1. Effect of temperature alone under atmospheric pressure.
2. Effect of repeated heating to high temperature and cooling to room temperature.
3. Effect of regeneration temperature and pressure as used under commercial conditions in adsorption plants.

All three types of investigations have shown a change from high order to low order diffraction patterns as temperature, pressure, and number of repeated heating and cooling increase, i.e., all three types investigations have shown a gradual gain in crystallinity.

It has been also possible for the first time, to correlate the effect of increased relative intensity of the different diffraction patterns with other variables, e.g., surface area, adsorptive capacity, in an empirical type of equations. Such equations can be used as a basis for future investigators to further explore this area.

ACKNOWLEDGMENT

The author wishes to express his gratitude and indebtedness to Dr. John M. Campbell, the Research Director of this work, for his guidance and constructive criticisms and careful review of this work; his sage advice was a steadying influence.

In addition, he wishes to express his appreciation to Dr. Charles Mankin, Geology Department, for his help and suggestions; and to his colleagues in the Natural Gas Laboratory and the members of the X-Ray Laboratory who were constantly ready to give assistance. Also to Mr. Rick Kingelin for his help in analyzing the empirical equations on the computer.

A fellowship from the United Arab Republic and a research fellowship from the Davison Chemical Company, Division of W. R. Grace Company, are gratefully acknowledged.

Finally, to my wife, Sameha, goes the bulk of my thanks. She was both mother and father to our children, and remained always in good cheer while her husband was busy preparing this dissertation.

TABLE OF CONTENTS

LIST OF TABLES

LIST OF ILLUSTRATIONS

LIST OF ILLUSTRATIONS
(Continued)

THE EFFECT OF REGENERATION TEMPERATURE AND PRESSURE ON THE ADSORPTIVE CAPACITY OF SILICA GEL IN A HYDROCARBON ENVIRONMENT

CHAPTER I

INTRODUCTION

Silica gel finds widespread application as an absorbent for water and/or hydrocarbons in the petroleum industry. Fixed bed units consisting of two or more towers are employed. Once a tower becomes saturated with the desired adsorbate(s), it is regenerated by passing hot gas through it for the purpose of "stripping" the adsorbate from the surface.

In the most common three tower plant, one tower is adsorbing, one is being regenerated and the third is being cooled. The exact means of accomplishing this mechanically varies from plant to plant. Regardless of the other differences, it is customary to regenerate at system pressure until the outlet gas temperature attains 450-500°F. Said pressure customarily varies from 400-1200 psig.

Silica gel is an amorphous solid which possesses a surface area of 200-800 square meters per gram by virtue of being honeycombed throughout with capillaries. From a thermodynamic viewpoint all the

amorphous materials are somewhat unstable. According to classical concepts, the physical state of a substance depends on a balance between the kinetic energy of the molecules and the potential energy of the forces of interaction that bind these same molecules (or atoms) together. This balance depends on both pressure and temperature. There is not as much difference between gases and liquids as between liquids and solids. Gases and liquids differ in that the potential energy of the latter has become a significant factor. We characterize this by means of density and viscosity. When the potential energy exceeds the kinetic, the system passes over to the solid state. The lowest possible particle energy (most ordered system) exists when said particles have an ordered symmetrical arrangement. Therefore all solids ultimately progress toward a crystalline structure.

Amorphous materials such as silica gel, although they are "solid" to the touch, are basically fluids with a very high viscosity. Given enough time at ambient conditions they too would become crystalline.

This raises the question as to whether or not use of elevated temperatures and pressures for regeneration of silica gel in commercial processes accelerates such crystallization to a measurable degree. Both temperature and pressure would potentially produce a more ordered arrangement based on both thermodynamic theory and past observations with other amorphous materials. Any such crystallinity produced would result in less surface area and less effective adsorption capacity. Such change would be additive with any other changes in surface characteristics or contamination by thermal cracking that inevitably occurs to at least some degree at elevated temperatures.

Past experience has shown that the adsorptive capacity of silica gel degrades with usage. It falls rapidly during the early life and then gradually levels out to produce a capacity versus time curve that has the general shape of a portion of parabola. In commercial units it is known that this degradation results from cracking of the heavier hydrocarbon molecules which "plug" the capillaries, heavy oils that cannot be easily regenerated (commonly called "heel"), and precipitation of sulfur and its compounds. One or all of these is present to some degree in any commercial unit. Consequently, it is customary to relate the effective life of any adsorbent bed to the level of such contamination present. Depending on this level, bed life will vary from a few months to five years, the average being about two years. Surprisingly enough, no formal consideration has ever been given to the possible role that regeneration temperature and pressure might play in the degradation. The primary purpose of this investigation has been to ascertain the effect of these parameters. A series of controlled tests were made in which all of the above factors normally considered to affect degradation have been minimized to a point that they could have no measurable effect on capacity. All runs were made with a lean natural gas containing over 99 percent methane which will not crack or form a significant film. Consequently, any significant change in adsorptive capacity would necessarily be dependent on a change in the basic structure of the silica gel. Precise measurement of pore size, surface area, and x-ray diffraction patterns of silica gel were made in order to have a quantitative picture of any changes in characteristics which might accompany a loss in capacity.

Knowledge of this behavior is of extreme importance to the petroleum industry. It would lead to a means of optimizing the regeneration portion of the cycle with a potential saving of millions of dollars in reduced heat requirements, silica gel costs and plant downtime.

CHAPTER II

PREVIOUS WORK

A great deal of attention has been focused on the mathematical models by which one may predict dynamic adsorption performance.[8,9,10,11,14,15,17,24,25,27] Almost none have been directed toward the effect of pressure and temperature on silica gel characteristics. Degradation of silica gel in service has been recognized but its inclusion in system design has at best been qualitative. Consequently it has been presumed (although never proven) that protection of the adsorbent from deleterious materials was the primary problem. It is interesting to note though that noticeable degradation occurred even when contamination did not appear to be a significant factor.

Silica Gel Behavior

Most of the X-ray diffraction work on silica gel has been performed either under vacuum or atmospheric pressure, at high temperature. The Debye-Scherrer camera or powder method [12] has been primarily used.

Patrick, Froyer, and Rush[34] determined that the capillaries in silica gel began to close when the gel was heated to 700° C.

Milligan and Hachford[29] made a study on the effect of elevated temperatures on silica gel having a surface area of 380 m^2/grm.

Samples were heated two hours at temperatures from 200° C to 1000° C; they reported that in no case did X-rays reveal any crystallization.

Kreger and Ries,[37] as well as Bastick,[3] believed that there is a growth of a crystalline phase at the expense of the amorphous dispersed phase.

Milliken, Mills and Oblad[30] noted that, with 2 per cent Al_2O_3, a gel which had been heated to 1000° C gave us a much stronger pattern of cristobalite than silica gel containing no alumina. On the other hand with still more alumina the cristobalite pattern became weaker. The most significant point is that small amounts of alumina greatly strengthen the cristobalite pattern in silica after the gel is heated to high temperature.

Racczwski and Richter[35] concluded that the SiO_2 in the silica gel had a sign of crystallization. Also Krejci and Ott[23] reported that freshly prepared silicic acid gels contained crystalline centers of colloidal dimensions.

Evidence of a change from the amorphous to a crystalline form has been evidenced although the exact mode and degree of such change has not been clearly defined. In a very general way this confirms the hypothesis that an amorphous material will ultimately become crystalline. It is simply a matter of what set of conditions will accelerate this process enough such that it becomes a matter of practical concern.

Dynamic Adsorption.

Physical adsorption is a reversible phenomenon, and is the result of intermolecular forces of attraction between molecules of the

solid and the substance adsorbed. From recent studies of the hydration and dehydration of silica it now seems fairly certain that the surface of silica gel is ordinarily covered with a monolayer of hydroxyl groups,[29] generally termed "bound water"; and that when silica gel is heated, this layer is partly removed without sintering the silica, leaving the surface negatively charged.

Michaels' approach has been used in this work to analyze adsorption performance because of its simplicity and it yields good results for both single and binary systems.[28] Its utility for characterizing the behavior of multicomponent gases is questionable, but served the purposes of this work.

Michaels used the principle of ion exchange which is essentially a chemical reaction between an electrolyte in solution and an insoluble electrolyte with which the solution is contacted. The mechanisms of these reactions and the techniques used to bring them about are analogous to adsorption.

The unsteady-state aspects of fixed-bed adsorption and the many factors which influence the adsorption make such computations for the general case most complicated. Michaels' simplified treatment is limited to adsorption from dilute feed mixtures, where the adsorption zone is constant in height as it travels through the adsorption column, and where the height of the adsorbent bed is large relative to the height of the adsorption zone. Many industrial applications fall within these restrictions.

Inasmuch as this approach will be used to analyze the results of this work, a detailed development of the method is included.

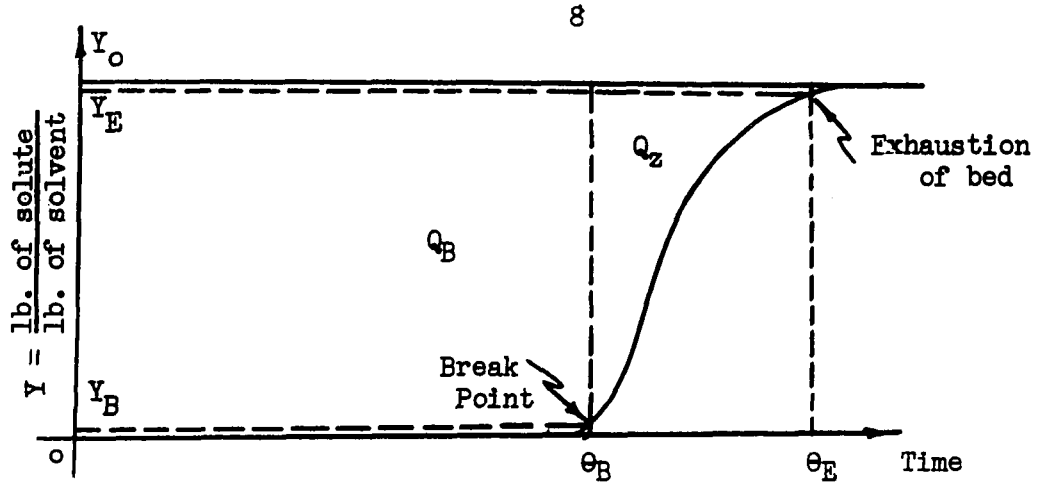

FIGURE A. Concentration of Adsorbent in Effluent versus Time.

Figure A represents an idealized breakthrough curve. This results from the flow of a solvent gas through an adsorbent bed, entering with an initial solute concentration Y_o. The breakthrough curve is steep, and the solute concentration in the effluent rises rapidly from essentially zero to that in the incoming gas. Some low value Y_B is arbitrarily chosen as the break point concentration, and the adsorbent is considered as essentially exhausted when the effluent concentration has risen to some arbitrarily chosen value Y_E, close to Y_o.

$$\theta_z = \frac{V_z}{V_g A} = \theta_E - \theta_B \qquad (1)$$

where θ_z = time required for exchange zone to move its own height down through bed under steady state conditions

V_z = volume of effluent during time θ_z

V_g = velocity of gas

A = total column cross sectional area.

Similarly, the time required, θ_E, for the zone to establish itself at

the top of bed and to move down out of bed is proportional to total volume of effluent collected V_E of

$$\theta_E = \frac{V_E}{V_g A} \tag{2}$$

Except for a period of time, θ_F, when the zone is forming at the beginning, the zone is descending through bed at constant rate determined by

$$V_Z = \frac{h_T}{\theta_E - \theta_F} \tag{3}$$

where: h_T = total height of bed

V_Z = velocity of zone front.

Therefore height of exchange zone $h_Z = V_Z \theta_Z$

$$h_Z = h_T \frac{\theta_Z}{\theta_E - \theta_F} \tag{4}$$

The only unknown is θ_F which is zone formation time.

During the passage of the zone, the quantity of hydrocarbon adsorbed from breakthrough to exhaustion of bed is

$$Q_Z = \int_{V_B}^{V_E} (Y_o - Y)\, dV \tag{5}$$

where: Q_Z = total amount adsorbed

V_B = volume of effluent collected to breakthrough

V_E = volume of effluent collected to dynamic equilibrium

Y_o = concentration of adsorbate in influent

Y = concentration of adsorbate in effluent

If the adsorbent in the zone had been substantially free of adsorbed components

$$Q_Z \text{ max} = Y_o V_z \tag{6}$$

Hence the fraction of adsorbent in the zone which possessed adsorption capacity is

$$F = \frac{Q_Z}{Q_{Z(\max)}} = \frac{\int_{V_B}^{V_E} (Y_o - Y)\, dV}{Y_o V_z} \tag{7}$$

If $F = 0$ very little material is adsorbed in the zone so it must have been well saturated.

Therefore $\theta_F = \theta_Z$

If $F = 1$ the zone must have been substantially unsaturated and the following relation satisfies this limit.

$$\theta_F = (1 - F)\, \theta_Z \tag{8}$$

Substituting θ_F in equation (4)

$$h_Z = \frac{h_T\, q\theta_Q}{Q_T} \tag{9}$$

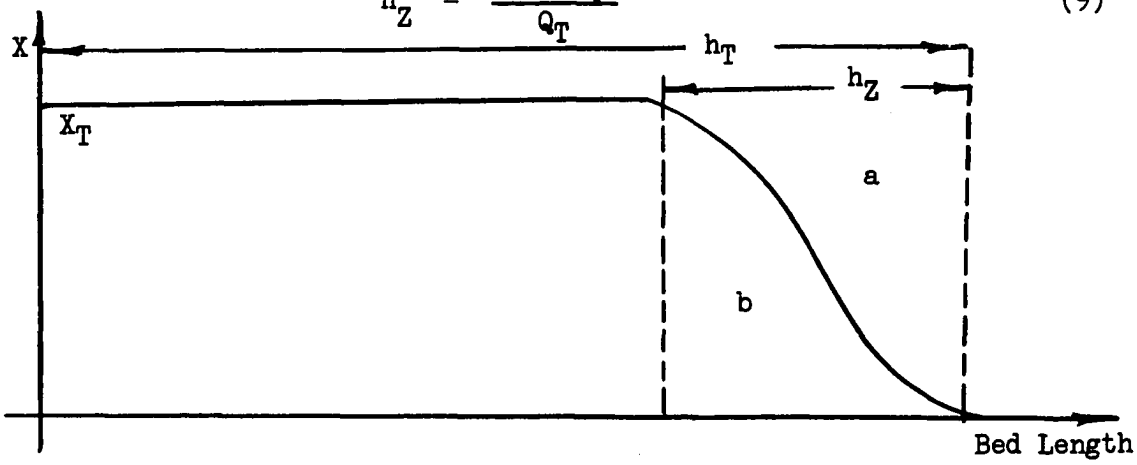

Concentration of Adsorbate Versus Bed Length

$$Q_T = Q_B + Q_Z = A\rho_B h_T X_T$$

where X_T = capacity of desiccant at saturation under the conditions of the run in question

= weight adsorbate per unit weight of desiccant

ρ_B = bulk density of desiccant

Q_B = total adsorbate on bed at breakthrough

Therefore

$$X_T = \frac{Q_T}{A_B h_T} = \frac{Q_B}{\text{Total Bed Wt.}} \quad \frac{\text{grm}}{\text{grm bed}} \tag{10}$$

Similarly

$$X_B = \frac{Q_B}{\text{Total bed wt.}} \quad \frac{\text{grm}}{\text{grm bed}} \tag{11}$$

X-Ray Diffraction

Inasmuch as X-ray diffraction plays a key role in the conclusions drawn from the data, a brief review of the pertinent knowledge is included.

X-rays are known to be electromagnetic radiations of exactly the same nature as light but of very much shorter wavelength. X-rays used in diffraction have wave lengths in the range of 0.5 - 2.5° A (°A = 1 x 10^{-8} cm), whereas the wave lengths of visible light is of the order of 6000°A.

Electromagnetic radiation, such as a beam of x-rays, carries energy. The rate of flow of this energy through a unit area perpendicular to the direction of motion of the wave is called the intensity I. In absolute units, the intensity is measured in ergs/cm^2/sec, but this measurement is inconvenient and most x-ray intensity measurements are made on a relative basis, in arbitrary units.(12)

X-rays are produced when any electrically charged particle of sufficient kinetic energy is rapidly decelerated. Electrons are usually used for this purpose. The radiation is produced in an x-ray tube which contains a source of electrons and two metal electrodes. The high voltage maintained across these electrodes, rapidly draws the electrons to the anode or target, which they strike with very high velocity. X-rays are produced at the point of impact and radiate in all directions.(21)

$$K.E. = eV = \tfrac{1}{2} mv^2$$

where: e = charge on electron

V = voltage across the electrodes

m = mass of electron (9.11×10^{-28} grm)

v = velocity just before impact.

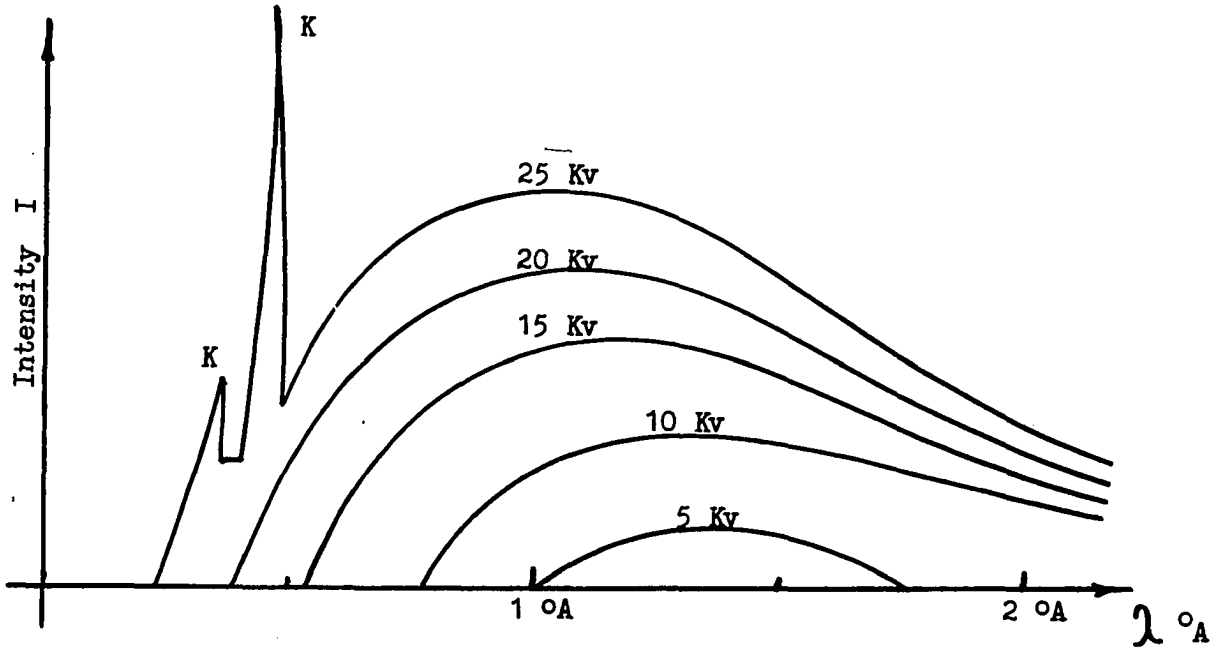

X-Ray Spectrum of Molybdenum Versus Voltage (Schematic)

When the rays coming from the target are analyzed,[12] they are found to consist of a mixture of different wave lengths, and the variation of intensity with wave length is found to depend on the tube voltage.

The smooth curves corresponding to applied voltages of 20 kv or less are called white or continuous radiations. On the other hand when the voltage on an x-ray tube is raised above a certain critical value, characteristic of the target metal, sharp intensity maxima appear at certain wave lengths, superimposed on the continuous spectrum called characteristic lines.

These lines fall into several sets referred to as K, L, M, etc. The K lines of a molybdenum tartet have wave lengths of about $0.7^{o}A$, the L lines about $5^{o}A.$, and the M lines still higher wave lengths. Ordinarily the K lines are useful in x-ray diffraction, the longer wave length being too easily absorbed.

The radiation from a copper target have been used to carry out this work due to the fact that at 30 Kv the K_{α} lines of a copper target have an intensity of about 90 times that of the wave length immediately adjacent to it in the continuous spectrum.

Laue, a German physicist (1912), reasoned that if crystals were composed of regularly spaced atoms which might act as scattering centers for x-rays, and if x-rays were electromagnetic waves of wave length about equal to the interatomic distance in crystals, then it should be possible to diffract x-rays by means of crystals.

Bragg, an English physicist (1913), later successfully analyzed the Laue experiment and was able to express the necessary conditions

for diffraction in a somewhat simpler mathematical form. Bragg defined a diffracted beam as a beam composed of a large number of scattered rays mutually reinforcing one another, i.e., in phase with one another. The diffraction essentially is a scattering phenomenon in which a large number of atoms cooperate. Since the atoms are arranged periodically on a lattice, the rays scattered by them have definite phase relations between them.

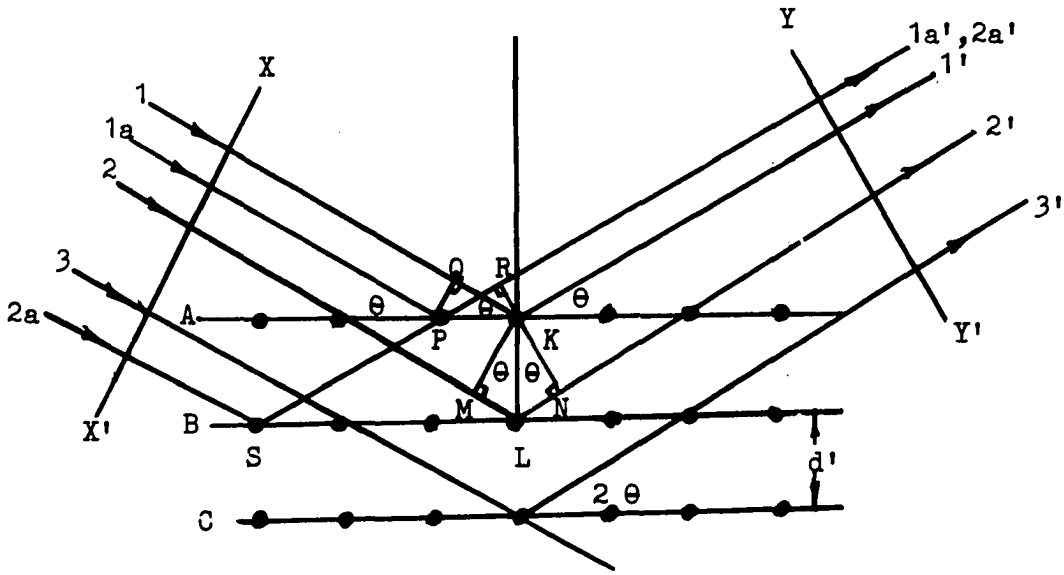

When a beam of x-rays strikes an extended crystal face and is reflected in the Bragg sense, the phenomenon is not a surface reflection, as with ordinary light. Parallel to the face is an effectively infinite series of equispaced atomic planes which the x-rays penetrate to a depth of several million layers before being appreciably absorbed. At each atomic plane a minute portion of the beam may be considered to be reflected. For these tiny reflected beams to emerge as a single beam of appreciable intensity, they must not be absorbed in passing through layers nearer the surface as they emerge. Far more importantly,

the beams from successive layers must not interfere and destroy each other. Bragg demonstrated these conditions in the following manner.

The previous figure shows a section of a crystal, its atoms arranged on a set of parallel planes A, B, C, D, perpendicular to the plane of the drawing and spaced a distance d' apart.(12) Assume that a beam of wave length λ is incident on the crystal at an angle θ, called the Bragg angle.

Consider rays 1 and 1a in the incident beam. They strike atoms K and P in the first plane of atoms and are scattered in all directions. Only in the directions 1' and 1a' will these scattered beams be completely in phase and reinforce each other. They do so because the difference in their length of path between the wave fronts XX' and YY' is equal to zero.(12)

$$QK = PR = PK \cos \theta - PK \cos \theta = 0$$

Rays 1 and 2 are also scattered by atoms K and L, and their path difference is

$$ML + LN = d' \sin \theta + d' \sin \theta$$

Scattered rays 1' and 2' will be completely in phase if this path difference is equal to a whole number n of wavelengths or if:

$$n\lambda = 2d' \sin \theta$$

Such a formula is called the Bragg Law.

Since sin θ cannot exceed unity

$$\frac{n\lambda}{2d} = \sin \theta < 1$$

$n\lambda$ must be less than 2d

For diffraction, the smallest value of n is 1 (because n = 0

corresponds to the beam diffracted in this same direction as the transmitted one and it cannot be observed). Therefore, the condition for diffraction at any observable angle 2θ is :

$$\lambda < 2d$$

Crystal Single Atom

A single atom as shown in the figure scatters an incident beam of x-rays in all directions in space, but a large number of atoms arranged in a periodic array in 3-dimensions to form a crystal, as shown in the figure, scatters (diffracts) x-rays in relatively few directions. It does so because the periodic arrangement of atoms causes destructive interference of the scattered rays in all directions except those predicted by the Bragg law. In these directions constructive interference (reinforcement) occurs.

The curve of scattered intensity I vs. 2θ for a crystalline solid is almost zero everywhere except at certain angles where high sharp maxima occur; these are the diffracted beams.

The non-crystalline solids have a structure characterized by a lack of periodicity which can usually be improved when such solids are subjected to a certain high temperature and pressure.

The liquids are characterized by an almost complete lack of periodicity. Finally there are the monatomic gases which have no structural periodicity whatever.

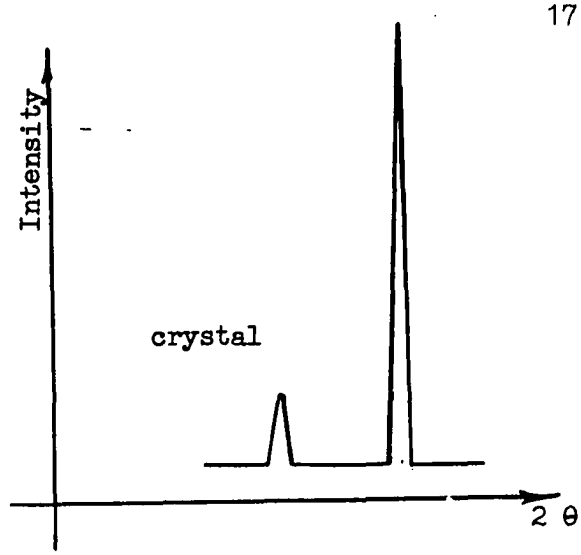

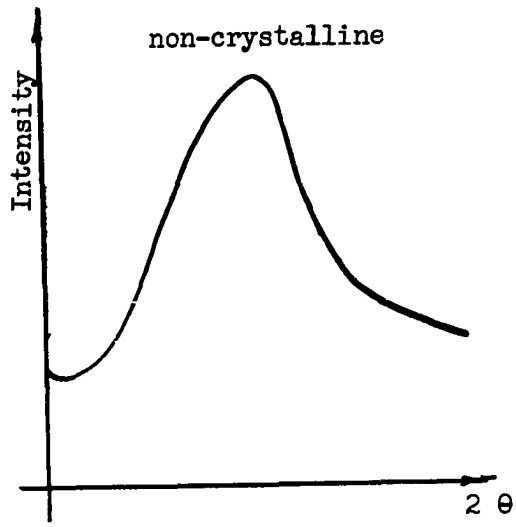

Silica gel can be classified under the non-crystalline solids since it gains at least some crystallinity when proper conditions of temperature and pressure prevail.

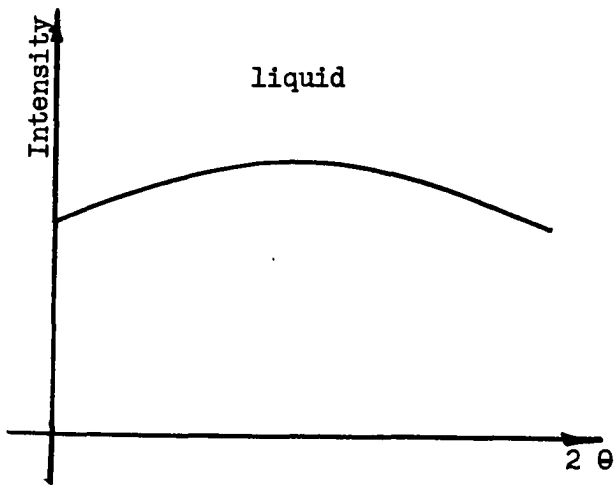

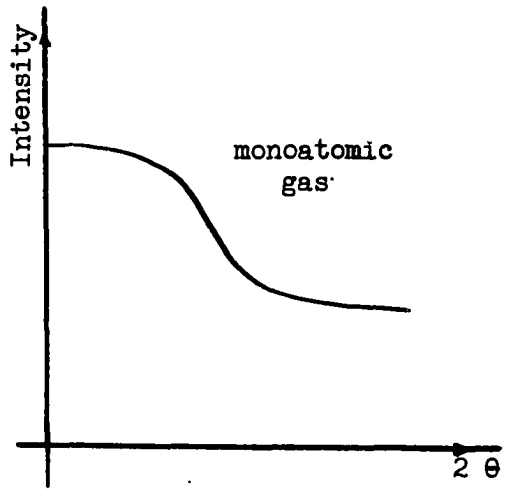

CHAPTER III

APPARATUS

The experimental portion of this work consists of 3 major subdivisions.

I - Adsorption measurements

II - X-ray diffraction analysis

III - Surface area and pore volume data

I - Adsorption

Adsorption measurements were performed in a carefully instrumented, pilot-sized adsorption unit where percentage error is less than 3%. The adsorption columns were 3 inches in diameter and could be varied in length from 4-15 feet. The gas used was taken from the Oklahoma Natural Gas Company line serving the City of Norman, Oklahoma; and compressed to the desired pressure by a 15,000 SCF per hour, compressor. Unloaders on the crank end allowed discharge reductions of 100%, 75%, 50% and 25%, permitting a wide range of gas flows to be used. The compressor is driven by a 60 H.P., 220 V, 3 phase electric motor.

The dry compressed gas is cooled to the desired temperature by sending it through the large coil of an air cooler. The gas is further cooled by passing it through a double pipe heat exchanger. Water is

cooled by a 100,000 Btu per hour cooling tower and is supplied to the tube side of the heat exchanger by a small centrifugal pump. The gas is then passed through activated carbon towers before it reached the adsorption towers.

A predetermined amount of liquid hydrocarbon is injected by a proportioning pump. Pumping rate is varied by either changing the length of the stroke of the plunger or changing the speed of rotation. Fluid injected by the pump is vaporized by a steam jacket and mixed with the gas prior to entering the adsorber.

Measurement of the gas flow rate was obtained with a standard orifice meter, utilizing flange taps and a high pressure water manometer to measure the pressure differentials.

The gas was analyzed with a CEC 26-212 gas chromatograph which can sample the emitted gas stream at desired intervals (2, 3, 4, etc. minutes). Temperatures in the towers were measured by thermocouples connected to a temperature recorder. A check on gas gravity was kept by means of Kimray gravitometer. (See Figure A for a complete flow sheet diagram).

To illustrate further the items discussed above, photographs showing various portions of the laboratory and related equipment are included as Figures (B) through (J).

II - X-ray Diffraction

The x-ray work was done by XR-6 diffractometer furnace and by the standard Norelco type diffractometer.

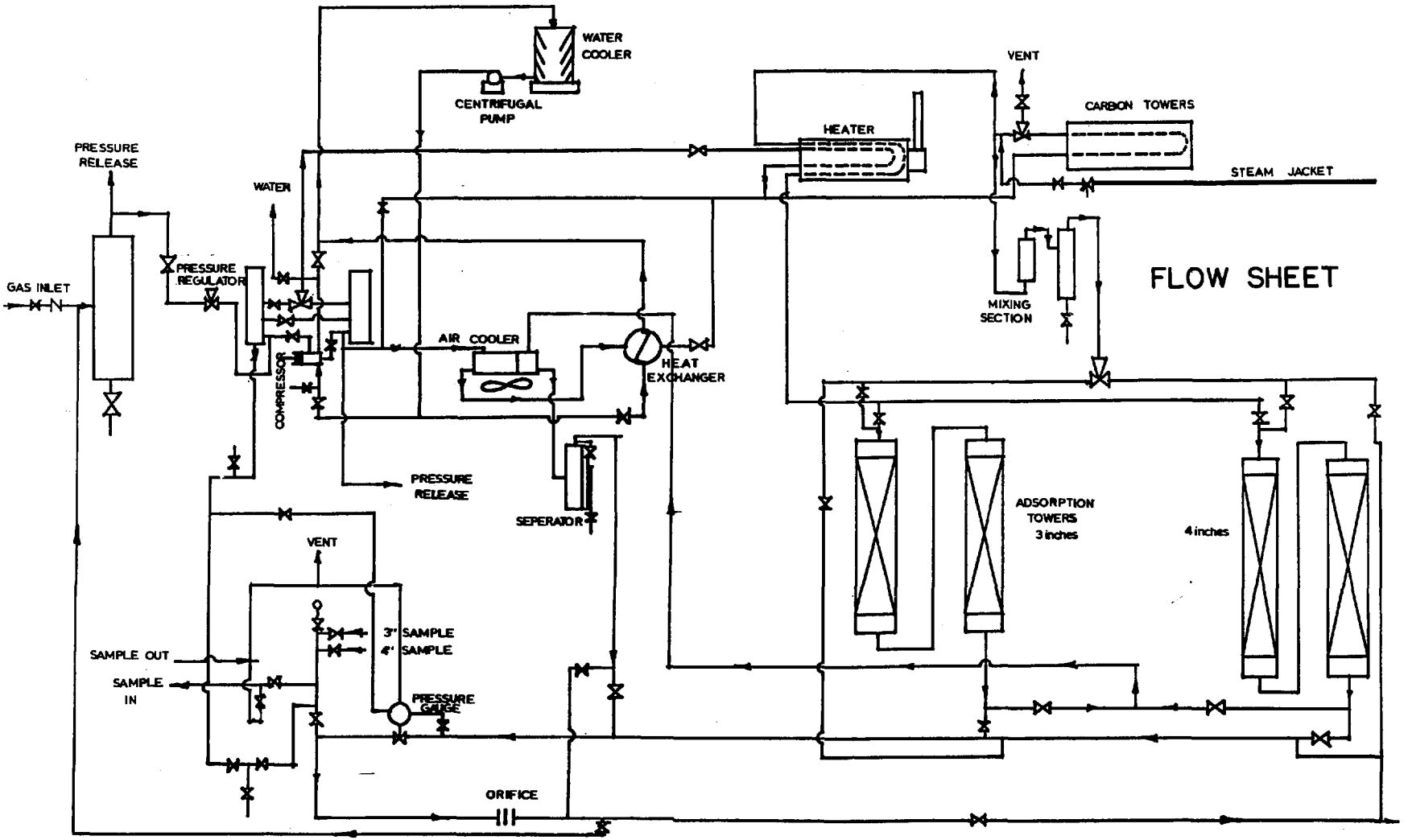
WATER COOLER
CENTRIFUGAL PUMP
VENT
CARBON TOWERS
HEATER
STEAM JACKET
PRESSURE RELEASE
WATER
FLOW SHEET
GAS INLET
PRESSURE REGULATOR
COMPRESSOR
AIR COOLER
HEAT EXCHANGER
MIXING SECTION
PRESSURE RELEASE
SEPERATOR
ADSORPTION TOWERS 3 inches
4 inches
VENT
3" SAMPLE
4" SAMPLE
SAMPLE OUT
SAMPLE IN
PRESSURE GAUGE
ORIFICE

FIGURE A

Natural Gas Laboratory
(B)

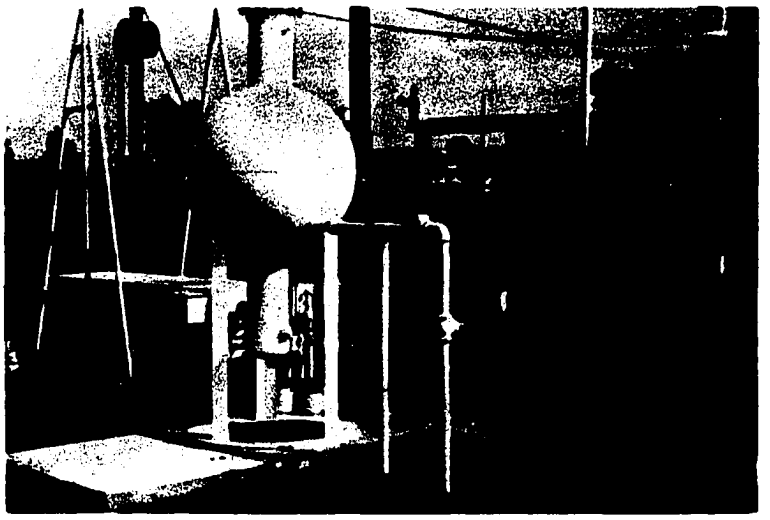

Carbon Tower
Salt Bath Heater
Gas Separator
(C)

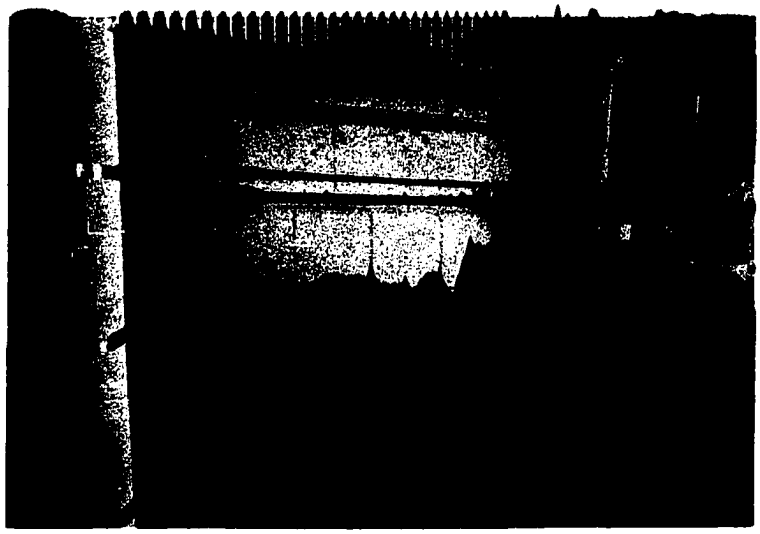

Fluid Injection Pump and Feed Tank
(D)

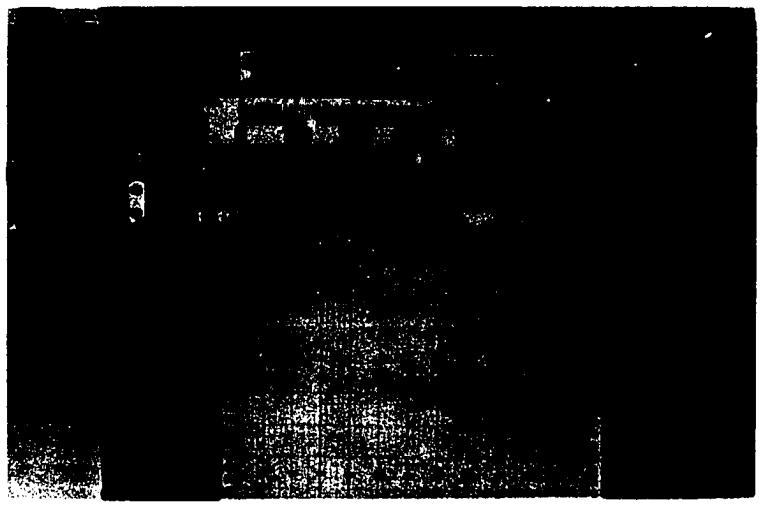

Temperature Recorder
(E)

Gas Chromatograph Analyzer
Kimray Gravitometer
High Pressure Water Manometer
(F)

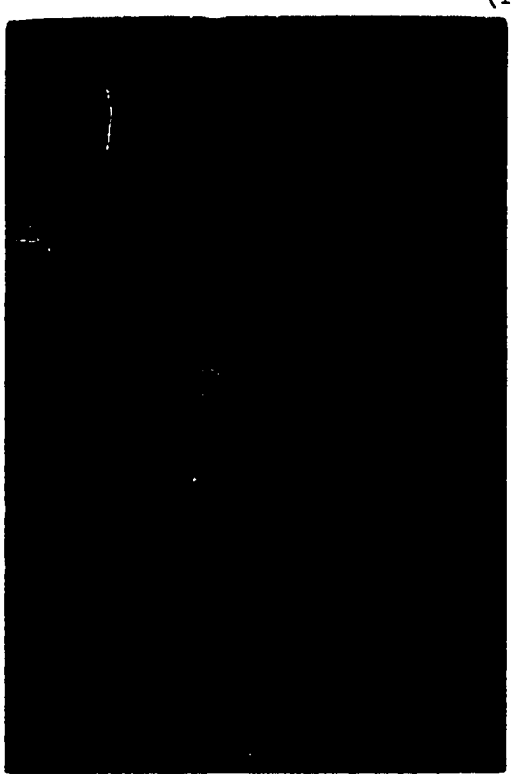

Adsorption Columns and
Mixing Unit
(G)

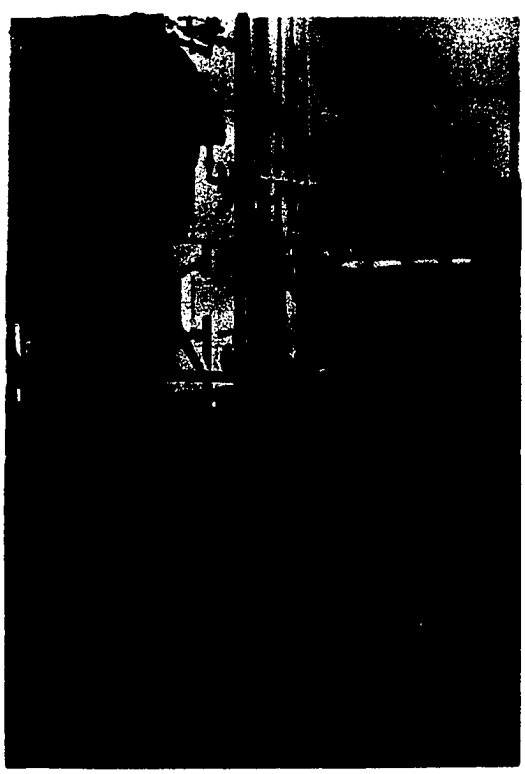

Gas Regulator
Air Cooler
Heat Exchanger

Gas Chromatograph CEC 26-212 Model

(I)

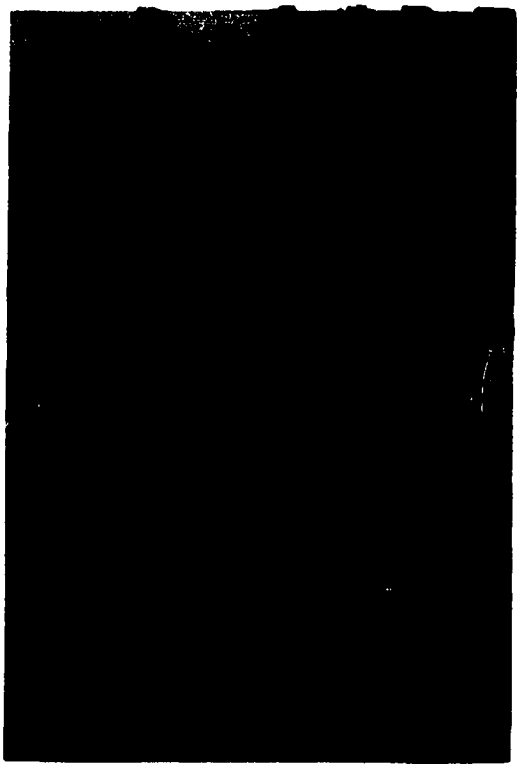

Compressor and
3-Phase Electric Motor

(J)

The basic function of both diffractometers are the same except that the former has a heating element in order to investigate the effect of temperature of the phase changes of the substance being investigated.

The following is a brief description of the x-ray diffractometers used in this work.

The Norelco type diffractometer and the XR-6 model furnace diffractometer consist of the following major parts:

1. Control
2. High voltage generator
3. Cooling system
4. Electronic circuit panel
5. High angle goniometer

1 - Control

It consists of a stepless variable auto-transformer operable under load, a continuously variable x-ray tube current control operable under load, an x-ray and rectified filament stabilizer including all necessary switches connectors. The high voltage can be varied from 0 to 60 KVP and the x-ray tube current from 2 to 50 Ma.

2 - High Voltage Generator

It consists of a high voltage transformer providing excellent regulation, two high voltage rectifier filament transformers, a high voltage x-ray filament transformer mounted in a single oil-filled water cooled tank. The high voltage end-grounded generator provides full-wave rectified high voltage up to 60 KVP at 50 Ma continuously.

3 - Cooling System

It includes a radiator located in the transformer tank, a solenoid valve, a high-flow-rate filter, a pressure regulator and high and low pressure-limiting switches, as well as connections for circulating cooling water through the x-ray tube.

4 - Electronic Circuit Panel

The complete assembly contains the following components (as arranged from top to bottom).

a. special electronic recorder
b. clock panel
c. scaler and rate meter
d. geiger counter and amplifier circuit power supply
e. overall stabilizer for high voltage generator.

The vertical steel cabinet contains:

a. an auto-transformer assembly which provides regulated and filtered 115 volt supply for the electronic circuits.
b. a special fan for circulating air built into the back of the cabinet.

5 - High Angle Goniometer

It is a high precision instrument for the direct measurement of the angular position (2 θ), and intensities of x-ray diffraction phenomena. The instrument consists of a rigid frame driven by an electric motor and appropriate controls.

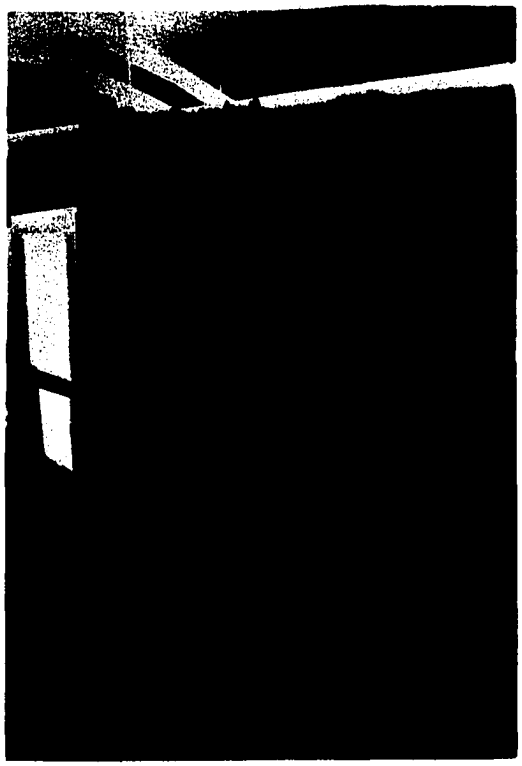

Norelco Diffractometer
(K)

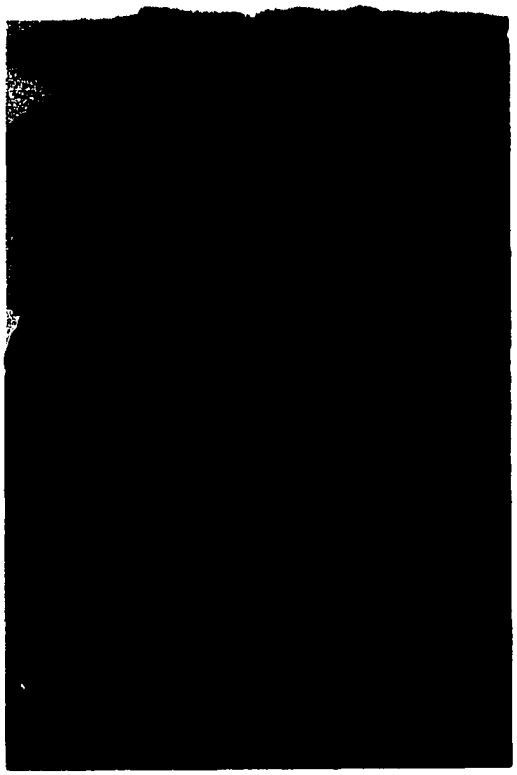

Recorder
(L)

High Angle Goniometer
(M)

Mounted to the goniometer are: the principal protractor, the detector, the soller slits, the defining and scatter slit assemblies, the filter and the specimen holder. The instrument is designed for supplying diffraction data within a Bragg angle range from -38° to 0 to 180° (2 θ°). The drive motor operating through the clutch and the worm transmission, provides for constant angular velocity of the main gear through either increasing or decreasing angles.

The XR-6 model has 3 groups of parts more than the Norelco type.

1 - Pressure (or vacuum) chamber which is mounted on

2 - Shaft - adjustment plate assembly

3 - Heater specimen plate which is mounted on the firewall inside of the pressure chamber.

The pressure chambes is chrome plated inside and out to provide the best possible heat reflection.

The mounting shaft is provided with a water-cooled barrier which keeps the shaft at room temperature. The pressure cap is held in place firmly by 3 knurled-head cap screws. Beryllium windows are mounted in the pressure cap with Teflon gaskets which permit diffraction angles from 0° to 140° (2 θ). The standard windows are only 0.03" thick.

To illustrate the items discussed above, photographs showing the various parts of the x-ray diffractometers are shown from Figures (K) through (O).

III - Surface Area and Pore Volume

This part of the work was performed in the W. R. Grace Company laboratories in Clarksville, Maryland, using conventional apparatus

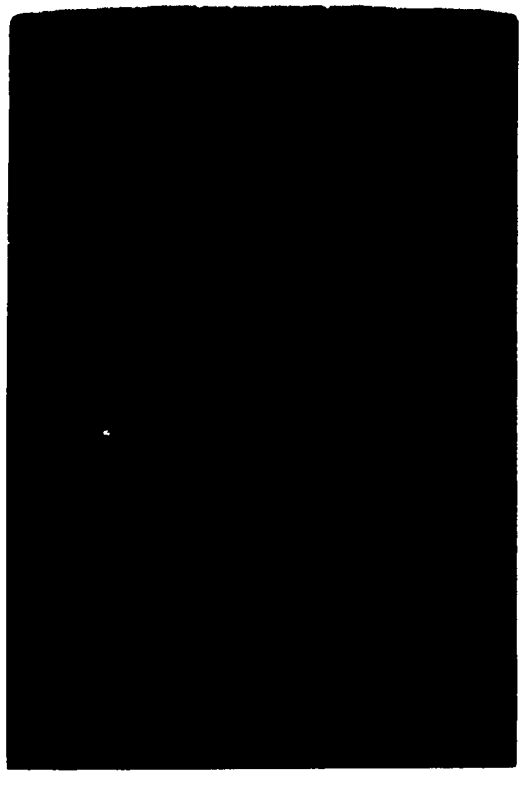

Control and
High Voltage Generator
(N)

XR-6 Furnace
Diffractometer
(O)

both surface area and pore volume measurements. They have one of the best equipped laboratories in the United States for work of this type and thus have a precision capability that far exceeds that of equipment available to the author.

CHAPTER IV

PROCEDURE

The following steps have been used to obtain the necessary data:

1. Five samples grade 3-8 mesh Davison silica gel were regenerated at 500°F. using available natural gas (mainly methane) for 40 cycles, at 1200, 1000, 800, 600 and 400 psi respectively, without adding any heavy hydrocarbons on the gel.
2. One sample has been regenerated for 80 cycles (as in Step 1) at 800 psi.
3. X-ray analysis has been performed on all samples prior to any heavy hydrocarbon injection.
4. Pore volume and surface area measurements were also carried on the gel prior to hydrocarbon injection.
5. All six samples used in Step 1 and 2 were subject to only <u>one</u> adsorption cycle using normal pentane (C_5H_{12}); and by keeping the variables affecting the dynamic adsorption constant.

Summary of Procedure

Each sample (about 17 pounds of silica gel) was placed in the 3-inch towers and heated to a temperature of 500°F to 520°F at different pressures; 1200, 1000, 800, 600 and 400 psi respectively. Temperatures

were recorded at regular intervals in the towers by the appropriate thermocouples.

Except for the first and last run of each series, when a controlled amount of n-pentane was adsorbed, all runs were conducted using a gas consisting of substantially pure methane (greater than 99 percent). Although the initial run could cause a small amount of film contamination, it would be common to all series of runs and would not affect the relative results.

When the exit temperature of the tower reached the desired regeneration temperature, valves on the tower were switched to cool the gel to about 100°F. Cycle time on each sample was kept as constant as possible (30 minutes). After 40 cycles of continuous heating and cooling, the sample was removed from the tower and replaced by another sample.

In order to investigate the effect of cycle number, a sixth sample of 03 Gel was kept in the tower for 80 cycles.

The total weight was recorded for each sample before and after the regeneration process as well as the height of silica gel in the tower. About 20-30 grams of each sample was kept for x-ray analysis and for specific surface area and pore volume measurements. The rest of the gel was sealed in a can and labeled with a symbol in order to be used in later adsorption runs.

Before starting the adsorption runs on the silica gel, each sample was regenerated to 500°F - 520°F, cooled to 100°F, saturated with the desired adsorbate (n-pentane), re-regenerated back and then cooled. The first regeneration was to remove the initial moisture content of the gel which varies between 4-7 per cent, and the second regeneration was

to clean the adsorbate from the gel. The regeneration process was performed by by-passing the towers and the effluent stream recycled through a salt bath bed heated to 500° - 600°F. (See Figure A). The hot gas entered the top of the tower to be regenerated and the extracted materials (water vapor or hydrocarbons) were passed through the small coil of the air cooler and the liquid trapped before the gas was vented to the atmosphere.

When the tower of silica gel was ready for the experiment, the temperature and the flow rate of the inlet gas stream were adjusted to desired values. Flow was then diverted from the column to the by-pass; the steam was turned on to help vaporize the injected hydrocarbon.

Gas samples from this rich stream were analyzed with the chromatograph, which was set on a three minute cycle. When the composition had been adjusted to the desired value, the flow was then turned to the main column and the adsorption experiment begun. Samples of the effluent gas from the columns were analyzed periodically to define the "break out" curve.

When the effluent gas composition had become identical to the inlet composition, and had remained at a steady value for several minutes, the experiment was terminated. Gas was continuously vented from the sampling header to insure a gas analysis which was representative of that flowing through the adsorber at any given time.

In order to investigate the effect of regeneration temperature and pressure on the adsorption capacity of the adsorbent, the parameters were kept as nearly constant as laboratory equipment permitted. The inlet temperature of the influent gas varied from 91.08°F to 94.2°F.

The tower pressure (P_B) and the orifice pressure (P_f) were very consistent in all the runs--800 psig and 105 psig, respectively. The amount of gas flowing through the towers (Q) varied from 2,765 to 2,772 SCF/Hr. The triplex pump gave good injection rates that varied from 41.86 grms/min to 42.68 grms/min of normal pentane. The velocity of the gas and the mole per cent of adsorbate were substantially constant from one run to the other. The velocity of the gas was 19.1 - 19.2 ft/min and the mole per cent of adsorbate ranged from 1.05 - 1.07 mole per cent.

X-ray Procedure

Two to four grams of silica gel were ground to 40 mesh with a plattner steel mortar, then ground to 80 mesh in a porcelain mortar. The sample was placed into the standard aluminum sample holder of the diffractometer. Diffraction spectra of each sample specimen were obtained. A preliminary evaluation of x-ray tube and counter types indicated that copper radiation and the scintillation counter were most efficient in producing and detecting silica gel spectrum.

Various scan rates, time constants and slit sizes were also tried. The following settings were used for all the patterns:

1 - multiplier - 1.0	2 - scale factor = 4 x 0.6 & 4 x 0.8
3 - time constant = 4.0 sec	4 - base line reading = 20.0
5 - window reading = 97.0	6 - operating voltage = 900
7 - KV = 35	8 - Ma = 18
9 - slit size = 1°	10 - chart speed ½" per minute

In contrast to the many sharp diffraction peaks from crystalline material, silica gel produces only a single broad peak on a strip-chart

recording. This peak will be referred to as the "maximum." The "maximum" corresponds in origin to the so-called diffraction ring that occurs on powder photographs. (No film work was done during the course of this study.)

Each silica gel sample was scanned three times between 14° and 32° (2 θ degree). Several characteristics of the resulting "maximum" were measured: areas (using planimeter), heights and widths of the different patterns, averaged over the three runs.

To investigate the effect of heating and cooling on the gel, a sample was heated in a furnace to 950°C and cooled to room temperature. After each cycle, the x-ray pattern was recorded. Finally the sample was left in the furnace for 4 days at 950°C and a last pattern was recorded after the sample had been cooled down to room temperature.

With the XR-6 model a sample was placed in the sample holder and the temperature increased from 200°C to 1000°C, at 100°C intervals. When the temperature stabilized in each case, the pattern was recorded.

Surface Area and Pore Volume Measurement (By W. R. Grace)

a) Surface area measurements were performed using the "Precision-Shell" apparatus based on the B.E.T. method (Brunauer, Emmett, Teller).[6]

A known weight of adsorbent was placed in a bulb connected to the necessary manometers, pressure gauges, etc. After the adsorbent was heated and evacuated, a known quantity of gas under test was admitted and brought to equilibrium with the adsorbent at a known temperature, and the pressure measured. If the volume of the bulb less that of the adsorbent (dead space) is known, the quantity of unadsorbed gas can be calculated and the amount adsorbed thus obtained.

b) Pore volume measurements: If a liquid of low volatility and viscosity is added slowly to an adsorbent, its free-flowing property remains while the liquid fills the microscopic pores through capillary forces, until all pores are saturated with fluid.

Water has been found to be an ideal agent for filling the pores of silica gel, resulting in a clearly-defined "caking end point."[18]

The apparatus consists of: a 4-ounce bottle; a burette (50 ml.) and a torsion balance.

$$\text{Pore volume} = \frac{A}{S} - 0.01 \text{ cc/grm.}$$

A = water used to reach end point, ml

S = weight of sample grms

0.01 = correction factor

cc/grm = estimated water required to bring about caking after pores are filled.

CHAPTER V

ANALYSIS OF RESULTS

This investigation is the first dynamic study of record which has isolated the variation of silica gel physical properties with time from the other factors causing degradation of capacity. Except for characterization runs at the beginning and end of the test period which used a gas containing pentane, all gas used consisted of substantially pure methane. This means that factors such as surface contamination, thermal cracking, sulphur deposition and the like were negligible. Furthermore, any such degradation for these reasons, however small, would be constant throughout the runs and would not affect the relative validity of the results.

The data clearly show that high regeneration pressures and temperatures affect the adsorptive capacity of silica gel. All, or most, of the degradation in capacity may be attributed to a basic change in the character of the silica gel.

Tables 1 through 6 (Appendix A) show the summary of data points (C/C_o versus time) obtained with the chromatograph, as well as the basic calculations of different parameters used for the computer program.

Figure 1 is a plot of (C/C_o) versus time for samples A, B, C, D, and F regenerated at 1200, 1000, 800, 600 and 400 psig respectively (for

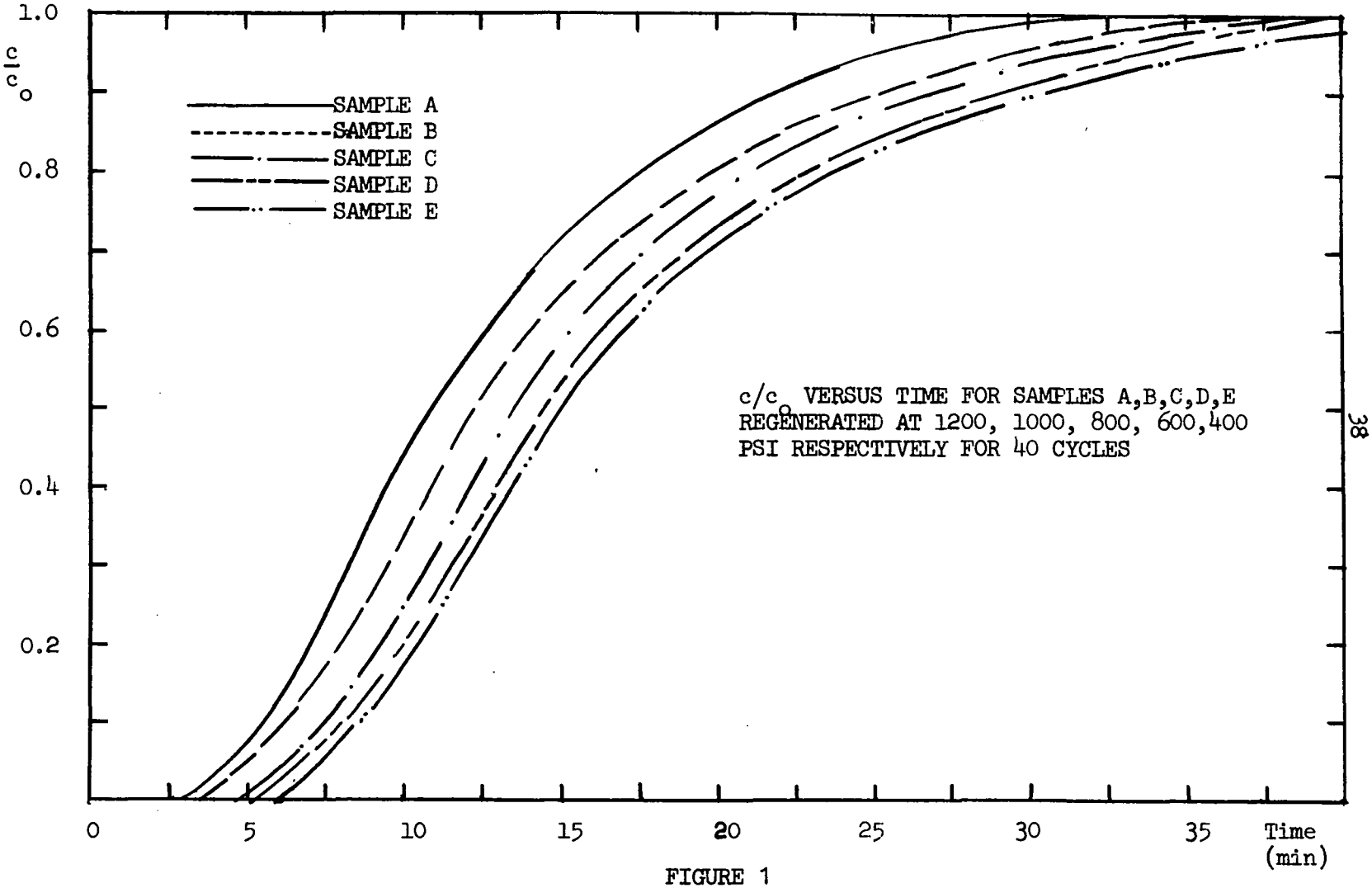
1.0
c/c_o
0.8
0.6
0.4
0.2
SAMPLE A
SAMPLE B
SAMPLE C
SAMPLE D
SAMPLE E
c/c_o VERSUS TIME FOR SAMPLES A,B,C,D,E
REGENERATED AT 1200, 1000, 800, 600,400
PSI RESPECTIVELY FOR 40 CYCLES
0
5
10
15
20
25
30
35
Time
(min)

FIGURE 1

40 cycles). This figure shows that sample A (regenerated at 1200 psig for 40 cycles) has an earlier break-through time (θ_B) and an earlier equilibrium time (θ_E) than the other four samples. A decrease in the values of θ_B and θ_E results in a corresponding decrease in Q_T. Consequently, Sample A has less dynamic adsorptive capacity than Sample B. By the same token, Sample B has less dynamic adsorption thatn Sample C, etc.

Figure 2 is a comparison between Samples C and F regenerated at the same pressure (800 psig) but for different number of cycles. Sample C was regenerated at 40 cycles and Sample F at 80 cycles. Sample C shows a better adsorptive capacity than Sample F, but the difference is not very pronounced. The difference in break-through time (θ_B) between the two samples was only 49 seconds. The equilibrium time (θ_E) varied only about 60 seconds. This probably indicates that in the early life of silica gel, regeneration pressure has much more effect on the gel than the number of reactivation cycles.

Table 7 (Appendix A) is a summary of results obtained. A general increase in both the break-through time (θ_B) and the equilibrium time (θ_E) is obtained as regeneration pressure decreases. This increase is also reflected in the capacity of the gel at break-through (X_B) and at saturation (X_T). From the results obtained it is also noted that Sample F which was regenerated to 80 cycles had less dynamic capacity than the same Sample C regenerated to only 40 cycles, as expected.

Figure 3 is a plot of time to break-through time (θ_B) and equilibrium time (θ_E) versus regeneration pressure after 40 cycles. The plot shows a gradual decrease in both values of θ_B and θ_E as regeneration pressure increases. In a common dynamic adsorption process, a decrease in

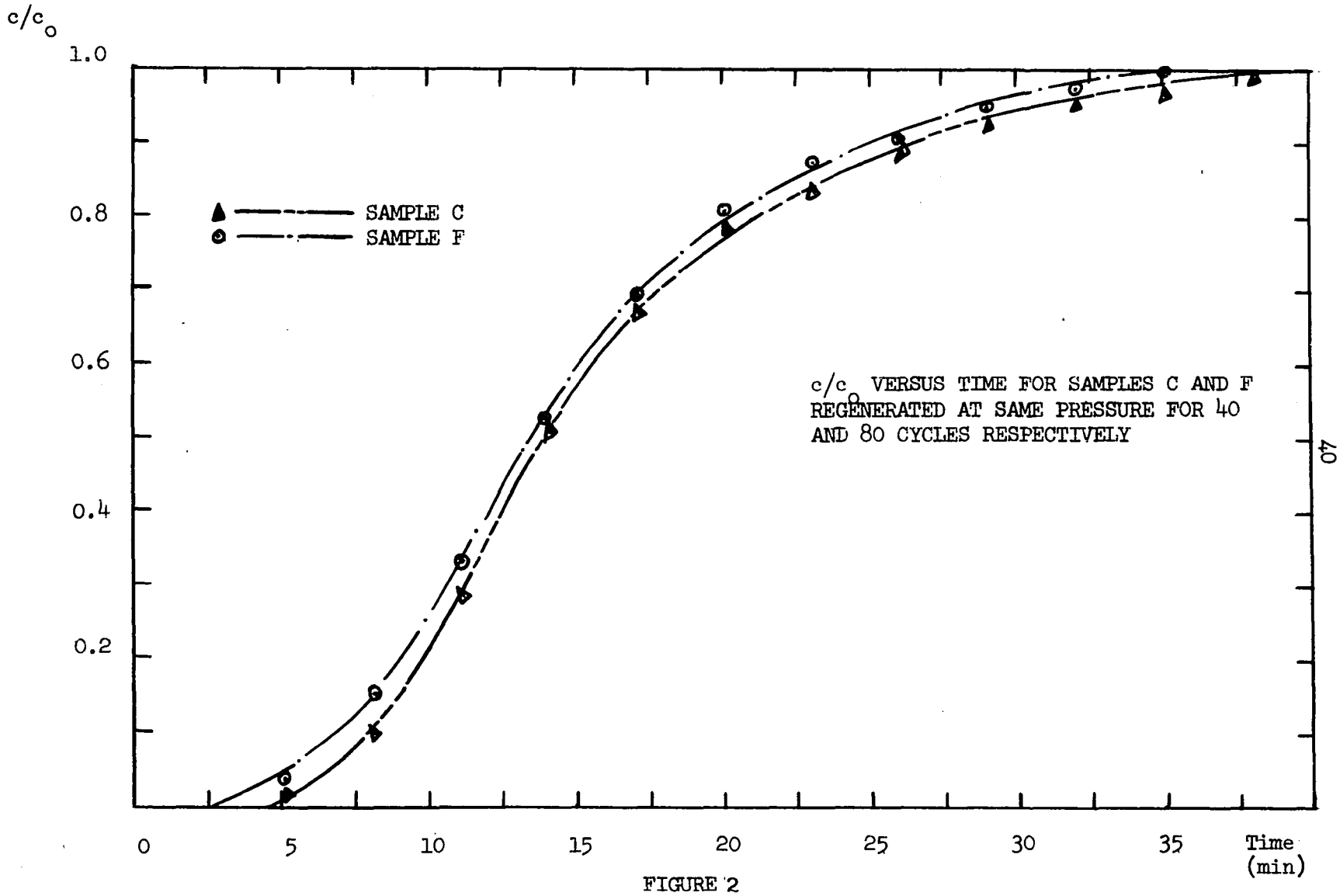
c/c_o
1.0
0.8
0.6
0.4
0.2
0
5
10
15
20
25
30
35
Time (min)
SAMPLE C
SAMPLE F
c/c_o VERSUS TIME FOR SAMPLES C AND F REGENERATED AT SAME PRESSURE FOR 40 AND 80 CYCLES RESPECTIVELY

FIGURE 2

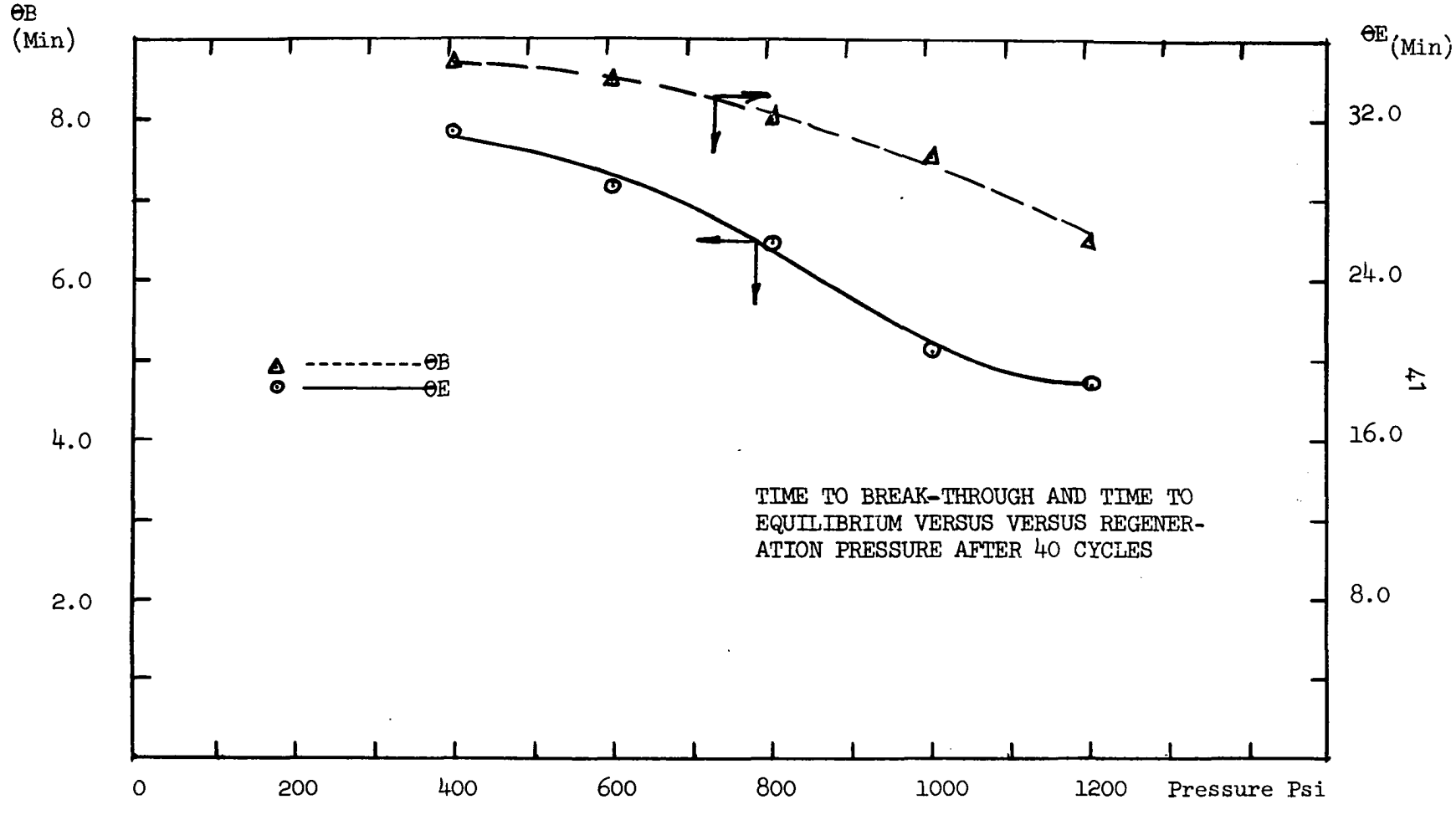
θB (Min)
θE (Min)
8.0
6.0
4.0
2.0
32.0
24.0
16.0
8.0
θB
θE
TIME TO BREAK-THROUGH AND TIME TO EQUILIBRIUM VERSUS VERSUS REGENERATION PRESSURE AFTER 40 CYCLES
0
200
400
600
800
1000
1200
Pressure Psi

FIGURE 6

θ_B or θ_E may be due to a change of one parameter or more which may affect the results. Since all adsorption experiments in this work were performed by keeping all variables (gas velocity, bed pressure, particle size, gas temperature, injection rate, etc.) constant, this decrease in the values of θ_B and θ_E may be attributed to regeneration pressure.

Figure 4 is a plot of the capacity of silica gel at break-through (X_B) and the capacity of silica gel at saturation (X_T), versus regeneration pressure after 40 cycles. It is noticed that the plot of X_B versus regeneration pressure has followed a reversed S-shape curve, with a small increase in the values of X_B in the interval of 1200-100 psig regeneration pressure and a rather high increase of X_B between 1000-800 psig. This is probably due to the same changes of θ_B at those pressures. The numerical value of X_B is related to θ_B by the following relation:

$$X_B = \frac{Q_B}{\text{total bed wt.}} = \frac{q\,\theta_B}{\text{total bed wt.}}$$

Hwnce at constant injection rate (q), a change in the value of θ_B will obviously cause a change in the value of Q_B. X_T versus regeneration pressure had nearly followed a straight line relationship up to a regeneration pressure of 700 psig. Such a relationship may be useful in predicting the value of X_T at any regeneration pressure within the interval 12o0-700 psig.

Figure 4(a) shows the variation of capacity with both adsorbent exposure and regeneration pressure. Only one series of tests was made beyond 40 cycles in order to ascertain the possible continued effect of time. Inasmuch as the number of cycles used is less than one per cent

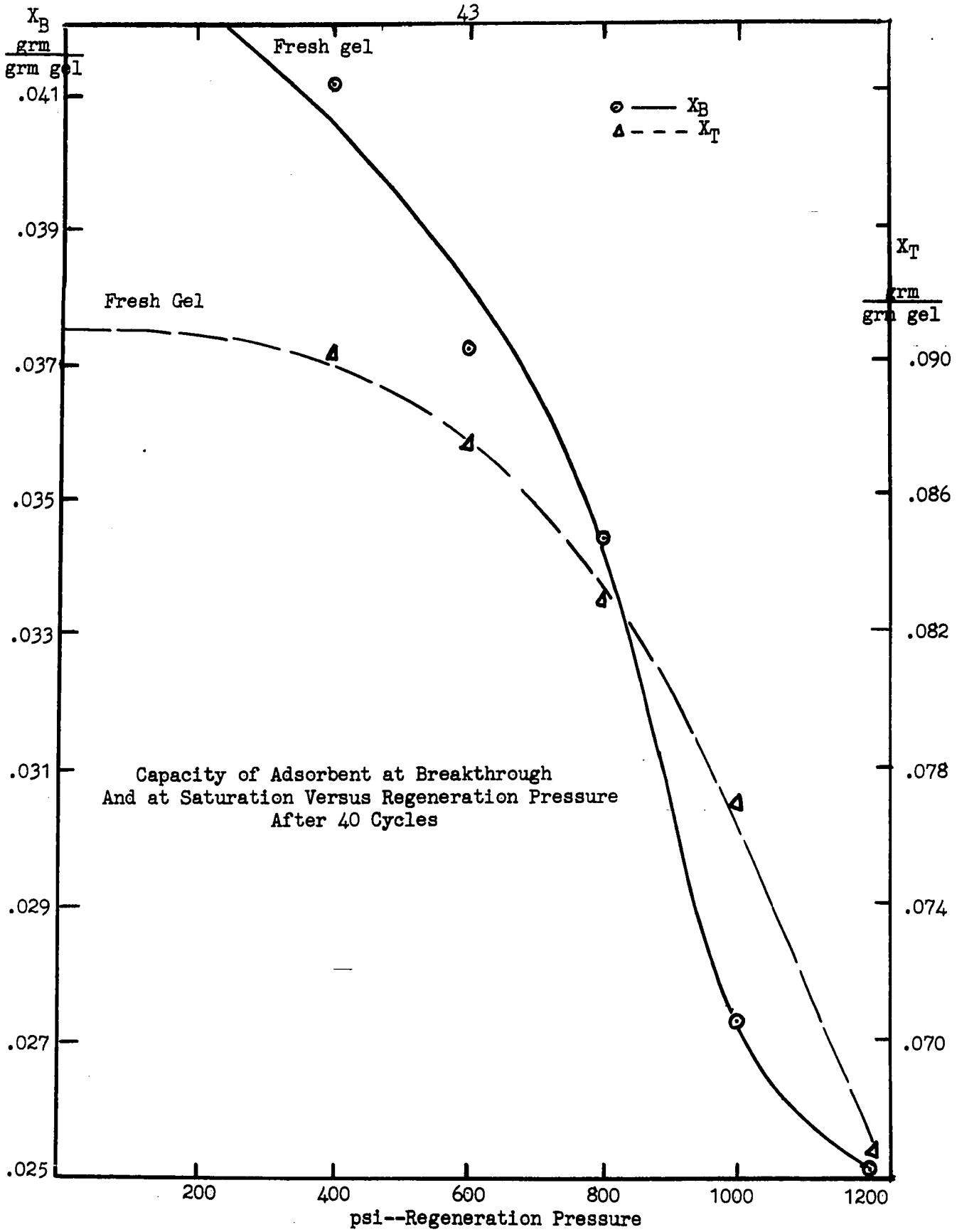
X_B grm / grm gel
Fresh gel
X_B
X_T
Fresh Gel
X_T grm / grm gel
.041
.039
.037
.035
.033
.031
.029
.027
.025
.090
.086
.082
.078
.074
.070
Capacity of Adsorbent at Breakthrough
And at Saturation Versus Regeneration Pressure
After 40 Cycles
200
400
600
800
1000
1200
psi--Regeneration Pressure

Figure 4

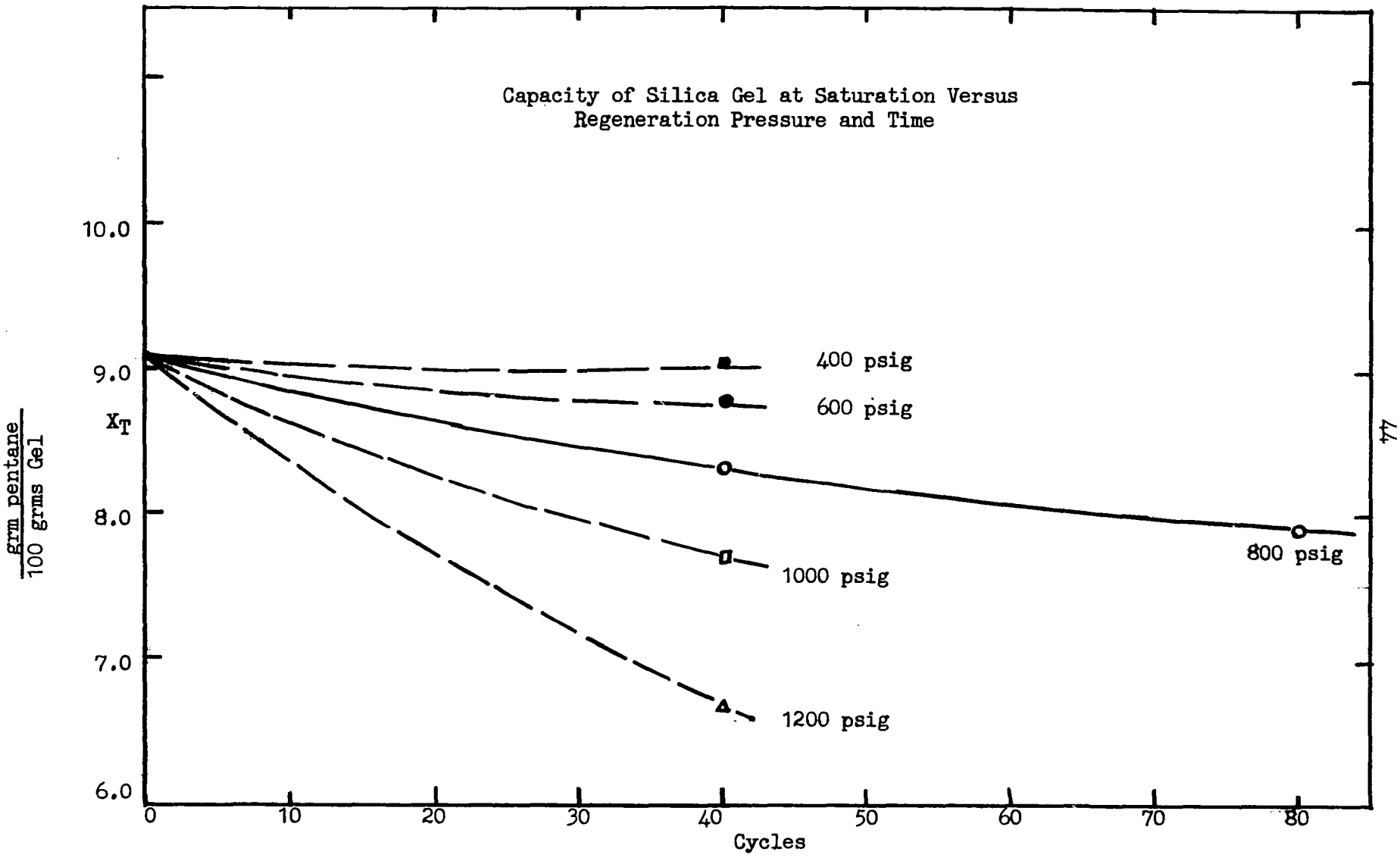
Capacity of Silica Gel at Saturation Versus
Regeneration Pressure and Time
10.0
9.0
8.0
7.0
6.0
X_T
grm pentane / 100 grms Gel
400 psig
600 psig
800 psig
1000 psig
1200 psig
0
10
20
30
40
50
60
70
80
Cycles

Figure 4(a)

of the total adscrption exposure during a year's use, the drop of about 11 per cent shown in this figure is significant. The change in slope with time is very gradual which indicates that the ultimate degradation in capacity is undoubtedly significant.

Table 8 (Appendix A) shows the data for surface area, pore volume and particle density of samples A, B, C, D and E. Figure 5 is the plot of data from Table 8. A gradual decrease in both surface area and pore volume values results as the regeneration pressure increases. These values seem to follow an asymptotic trend as regeneration pressure increases which probably means that at very high regeneration pressure, the effect of pressure will be substantially less.

Inasmuch as the loss in capacity was accompanied by corresponding losses in surface area and pore volume while the particle density increased, it appears that they are interrelated. Figure 5(a) clearly shows that surface area is truly dependent on exposure time and pressure. The cross-plot of the data shown in Figure 5(b) shows capacity is a function of surface area and pore volume. Since the 80 cycle data fall on the same smooth curve with the 40 cycle data, it would appear that any combination of time and pressure that caused a given reduction in surface area would yield a given capacity for the material studied.

The data shown in Table 8 confirm the logical conclusion that pore volume and surface area are dependent variables and that either may be used to characterize gel behavior with pressure and time. Development of a model that would express the relationship of these variables with regeneration pressure, capacity and time would require a long range study beyond this or any single other thesis. However, it has been

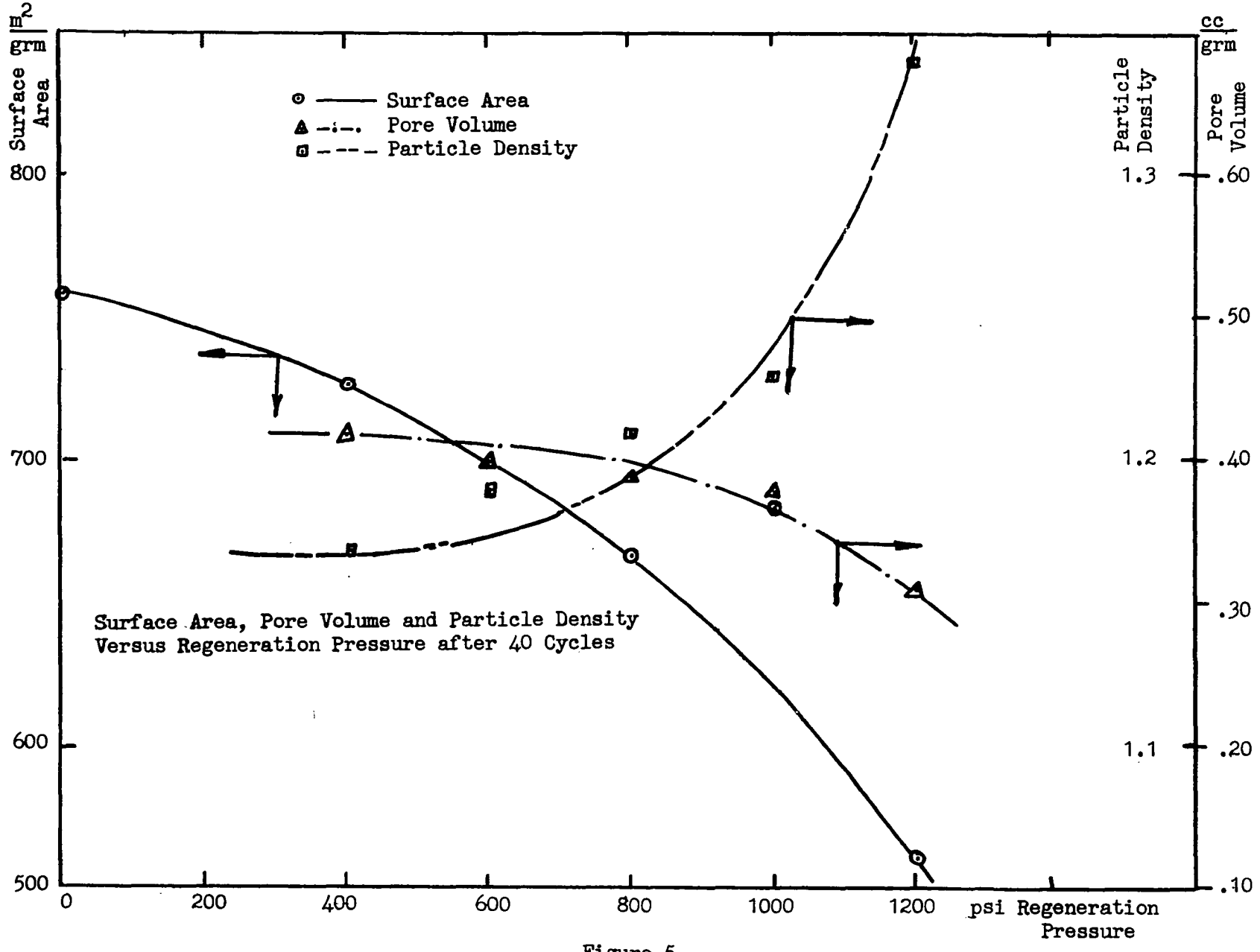
Surface Area
Pore Volume
Particle Density
Surface Area, Pore Volume and Particle Density
Versus Regeneration Pressure after 40 Cycles
Surface Area grm m2
Particle Density
Pore Volume cc/grm
800
700
600
500
1.3
1.2
1.1
.60
.50
.40
.30
.20
.10
0
200
400
600
800
1000
1200
psi Regeneration Pressure

Figure 5

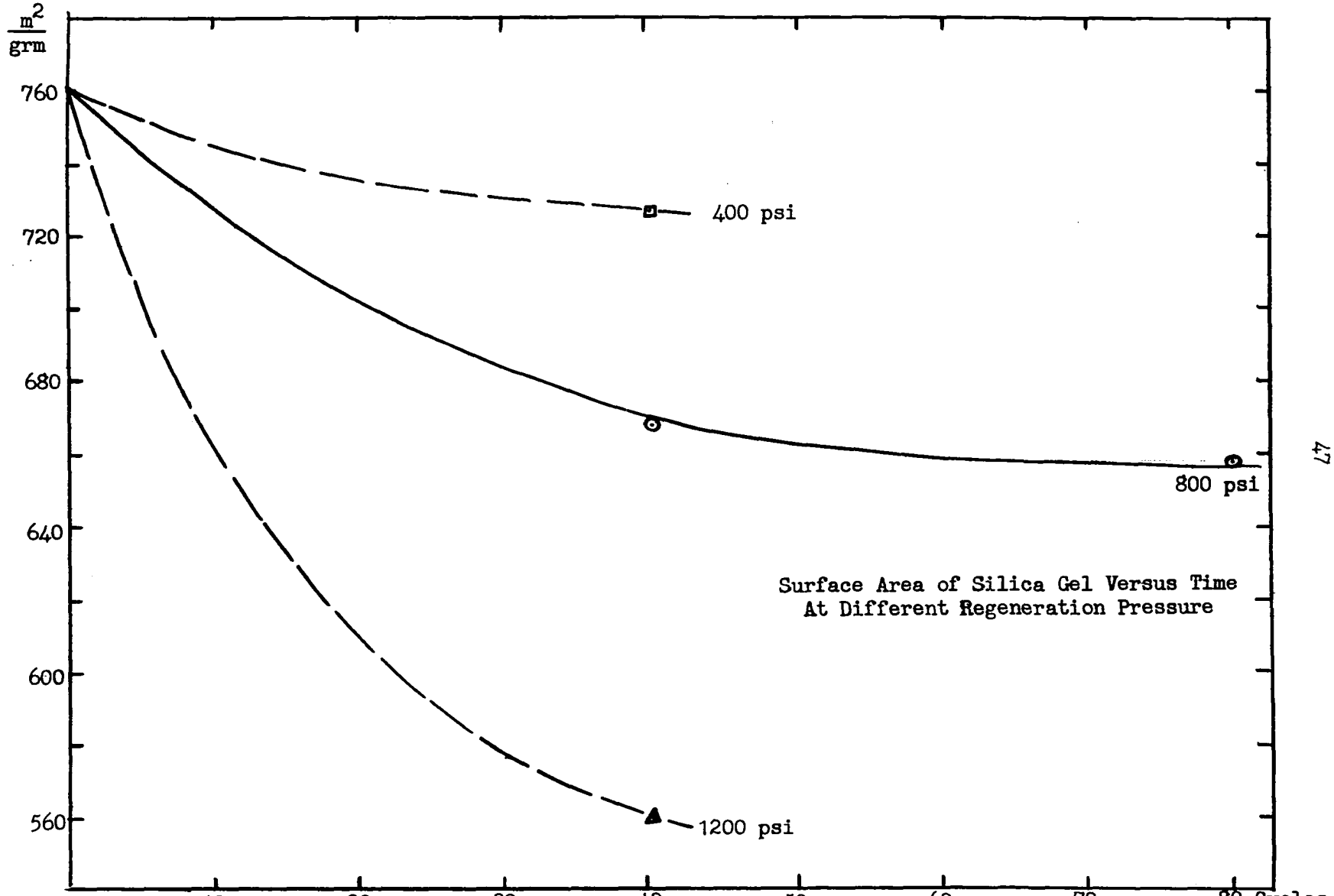
$\frac{m^2}{grm}$
760
720
680
640
600
560
400 psi
800 psi
1200 psi
Surface Area of Silica Gel Versus Time
At Different Regeneration Pressure
0
10
20
30
40
50
60
70
80 Cycles

Figure 5(a)

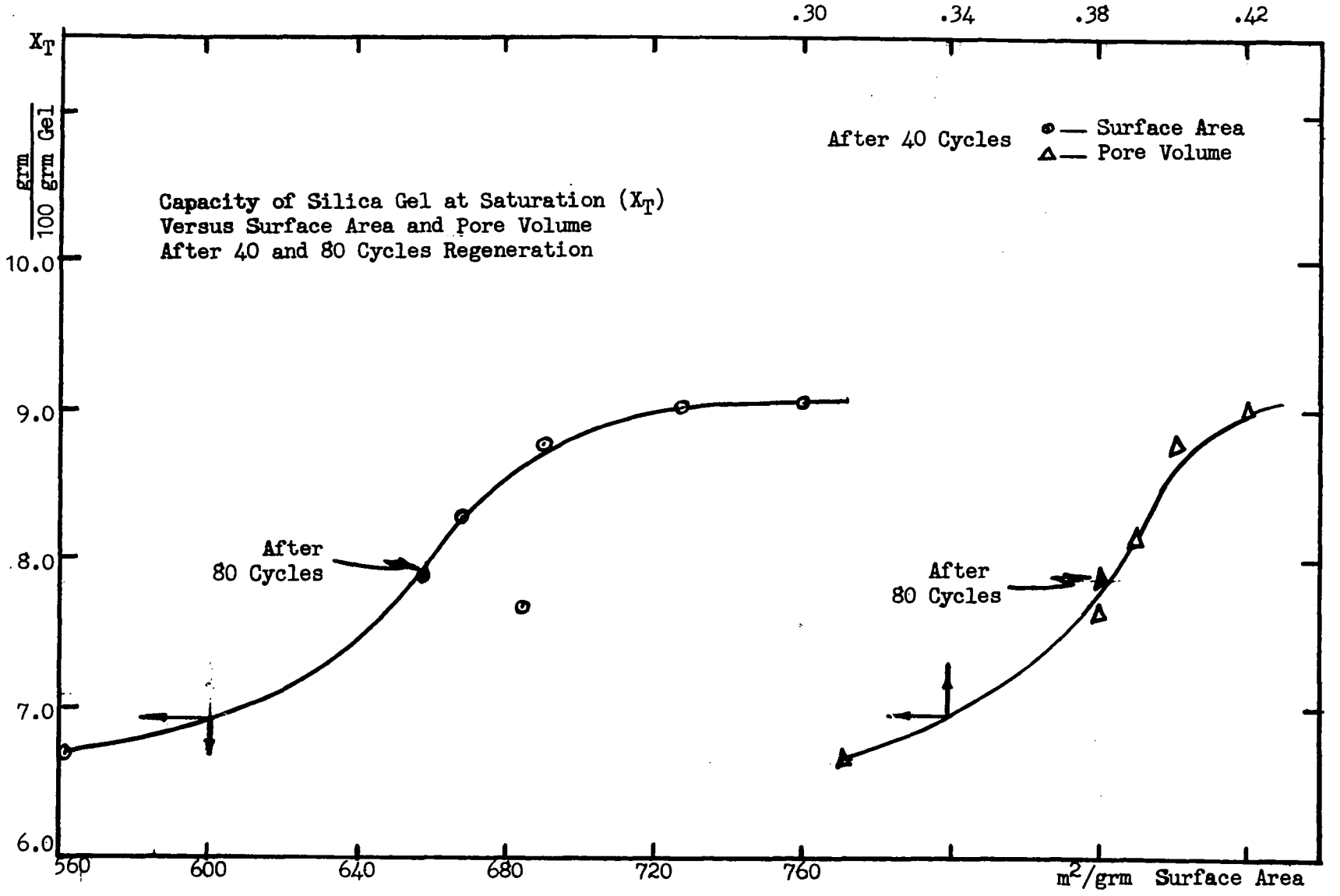
.30
.34
.38
.42
X_T
grm / 100 grm Gel
After 40 Cycles
Surface Area
Pore Volume
Capacity of Silica Gel at Saturation (X_T)
Versus Surface Area and Pore Volume
After 40 and 80 Cycles Regeneration
10.0
9.0
8.0
7.0
6.0
After
80 Cycles
After
80 Cycles
560
600
640
680
720
760
m^2/grm Surface Area

Figure 5(b)

possible to develop a series of equations that relates X_T with the several pertinent parameters at 800 psia regeneration pressure. These in turn permit one to relate the variables with each other.

The following equations were developed, by the polynomial curve fitting using the least square method:

$$X_T = 0.098 - 0.0006575\ (N_c) + 9.25 \times 10^{-6}\ (N_c)^2 - 5.0 \times 10^{-8}\ (N_c)^3$$

where N_c = number of regeneration cycles to 500°F at 800 psia.

$$X_T = 0.307 - 5.4 \times 10^{-4}(S.A.) - 1.04 \times 10^{-6}(S.A.)^2 + 2.36 \times 10^{-9}\ (S.A.)^3$$

where S.A. = surface area in m^2/grm.

$$X_T = 1.106 - 3.69(P.V.) - 5.47(P.V.)^2 + 7.12(P.V.)^3 + 51.08(P.V.)^4 + 62.0P.V.)^5 - 260.0(P.V.)^6$$

where P.V. = pore volume in cc/gram.

Inasmuch as pressures in the vicinity of 800 psia is very common, the above equations furnish a means of estimating the effect of the parameters shown on each other.

The x-ray diffraction portion of this study provided a valuable insight into the specific causes of the above noted changes.

Table 9 through 11 (Appendix A) summarize the results of x-ray diffraction work. It may be noted from these tables that when the re-activation pressure of the gel increases, the peak height and the area under the patterns increase (see Figures 7 through 11). On the other hand, the width of the patterns (W) at hilf maximum intensity increases

when regeneration pressure decreases. In normal x-ray diffraction interpretation a broad flat pattern denotes a non-crystalline case and lack of periodicity. On the other hand, a steep narrow peak reflects the existence of a crystalline substance.

Figure 5(c) shows that the relative intensity of the x-ray diffraction patterns appears to be a continuous function of gel surface area. Figure 6 shows the relationship with relative intensity and width of the patterns obtained. These data enable one to expand the number of characterizing parameters. It was also found that

$$\frac{I}{I_o} = -32.4 + 7.66(S.A.) \times 10^{-2} + 4.48 \times 10^{-5}(S.A.)^2 - 7.5 \times 10^{-8}(S.A.)^3 - 2.47 \times 10^{-10}(S.A.)^4$$

$$X_T = 0.055543 + 0.126611\ (I/I_o) - 0.115098\ (I/I_o)^2$$

The standard deviation in the previous equations vary vrom 0.01 to 0.05. The ability of the x-ray diffraction apparatus to quantitatively show changes in crystallinity, and the systematic changes in these patterns with the other variables shown above, makes it evident that the decrease in capacity is accompanied by accelerated rate of crystallization of the amorphous gel.

The effect of repeated heating and cooling of the gel at atmospheric condition was investigated. Figure 10 shows the different patterns of silica gel recorded on the x-ray diffractometer after 7 cycles, i.e., after the sample has been heated to 950°C and then cooled to room temperature seven times. Not much difference is noticed in the patterns after cycles 1 and 2; after cycles 3 and 4, the gel has shown some

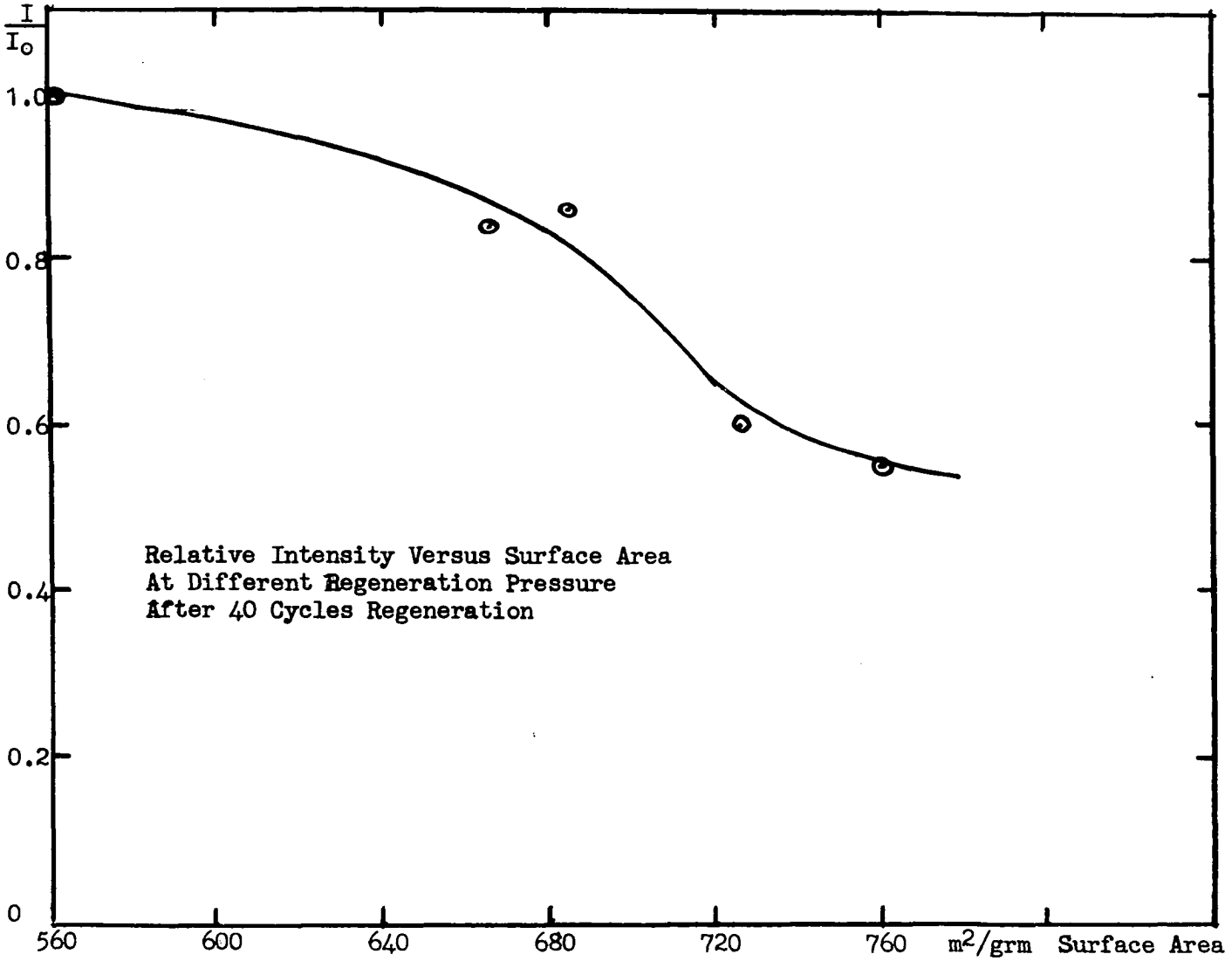
I/Io
1.0
0.8
0.6
0.4
0.2
0
560
600
640
680
720
760
m²/grm Surface Area
Relative Intensity Versus Surface Area
At Different Regeneration Pressure
After 40 Cycles Regeneration

Figure 5(c)

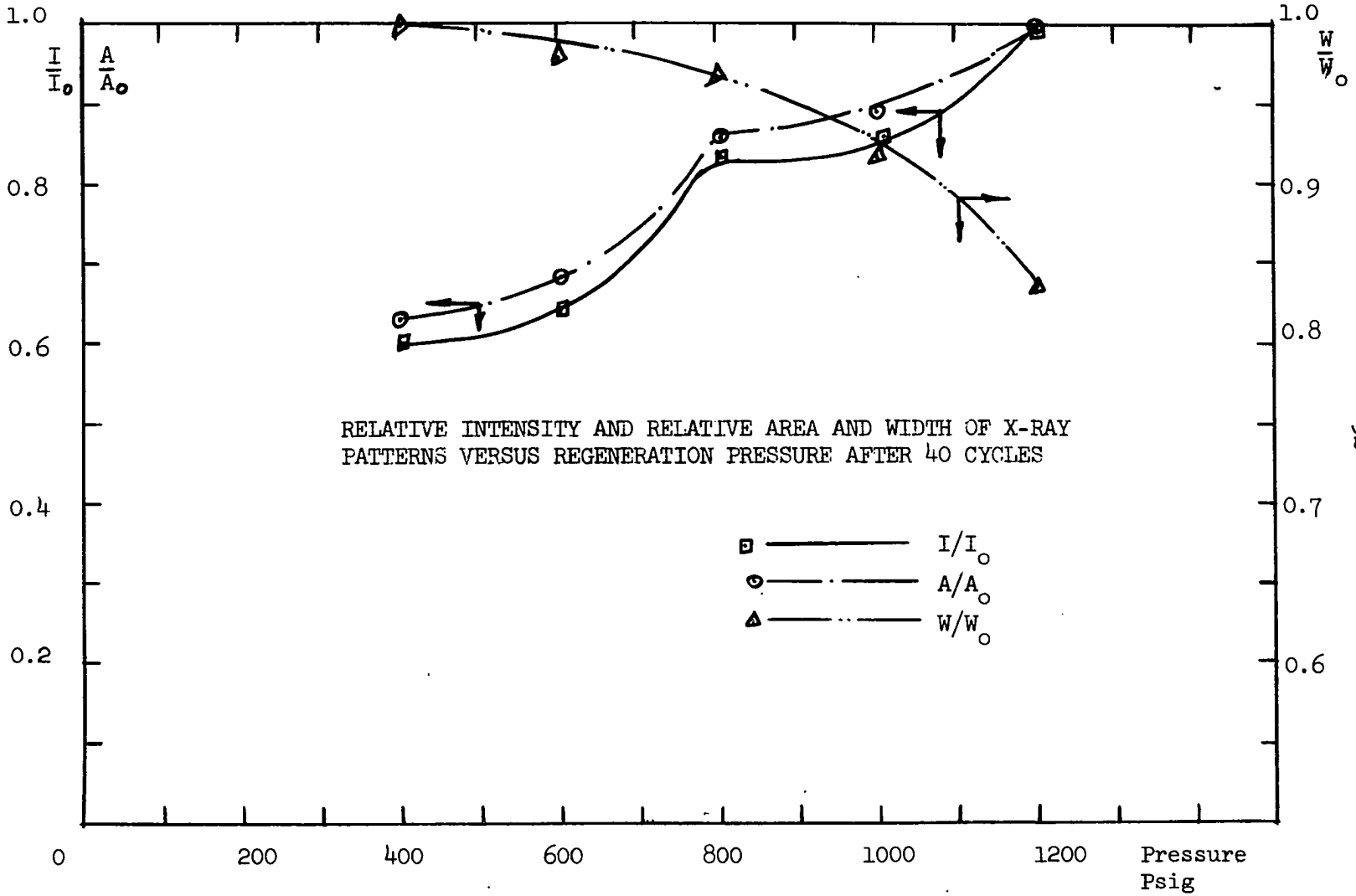

RELATIVE INTENSITY AND RELATIVE AREA AND WIDTH OF X-RAY PATTERNS VERSUS REGENERATION PRESSURE AFTER 40 CYCLES

FIGURE 6

increase in crystallinity. During cycles 5 and 6, the growth of the crystal was noticed at an angle $2\theta = 21.8^{9}$. A relative decrease in the width of the patterns was also obtained. During cycle 7, the sample was left in the fornace for 4 days at 950°C. The recorded pattern after cycle 7 has proven that the gel has been heated enough to show a clear peak at an angle $2\theta = 21.8^{\circ}$, and that an improvement of the structural regularity of the crystals has occurred in such a way that some of the x-ray diffracted beams are in phase, i.e., reinforcing one another, at an average "d" spacing = 4.05 °A.

If after 7 cycles the gel has gained some crystallinity, such a gel is also expected to gain more crystallinity when used under adsorption plant conditions: for 4000-5000 cycles under 600-1000 psi.

This proves that pressure and temperature above a certain range cause the molecules to become mobile enough to align themselves in accordance with the demands of crystal growth. In other words pressure and temperature cause silica gel to change from a high order diffraction pattern to lower order ones, i.e., from a high number of "d" spacing arrangements to a less number of "d" spacing which in turn helps reinforcing the diffracted beams of x-ray in accordance with the Bragg law of diffraction.

The identification of the formed crystal when silica gel is subject to repeated heating and cooling under high pressure is difficult due to the complicated phase relations of silica gel, which contains about 99.71% SiO_2. Under atmospheric condition "low-quartz" is formed at about 573°C and "high-quartz" is formed at temperatures between 573°C and 870°C. Over 870°C and up to 1470°C "tridymite" is formed.

On heating "high-quartz" to about 1670°C, it melts and the liquid produced would tend to crystallize to "cristobalite." (See reference 14a).

Since, in the commercial preparation of silica gel the amorphous state is usually produced by cooling the melt (1670°C) rapidly, where the internal friction increases so greatly that the molecules are unable to form a crystalline lattice; and from the available results of the x-ray patterns, we can conclude that the formed crystal is likely x-cristobalite which is formed at a Bragg angle $2\theta = 21.8^{9}$.

Figures 7-11 illustrate the above principle applied to the subject investigation. Three runs are shown for each condition to illustrate the reproducibility of this measurement. As regeneration pressure increases, the average "d" spacing decreases due to an increase in the Bragg angle.

Effect of Temperature Only

In order to investigate the effect only of temperature on the adsorptive capacity of silica gel, the XR-6 furnace was used at atmospheric pressure. It was noticed that up to 400°C (Figure 12) the temperature has almost no effect on the gel, i.e., the width (W) at half maximum intensity seems to be the same. This basically confirms operating experience which indicates little if any temperature effect on performance to 600°F. At 700°C and atmospheric pressure (Figure 14), silica gel shows a gradual increase in crystallinity and a decrease in the value of (W). Such crystallinity increases with the increase of heating on the gel till 1000°C is reached.

Figure 18 is the recorded pattern of silica gel when it was heated to 1000°C and left to cool down overnight at room temperature

EFFECT OF TEMPERATURE AND PRESSURE ON SILICA GEL DIFFRACTION PATTERNS

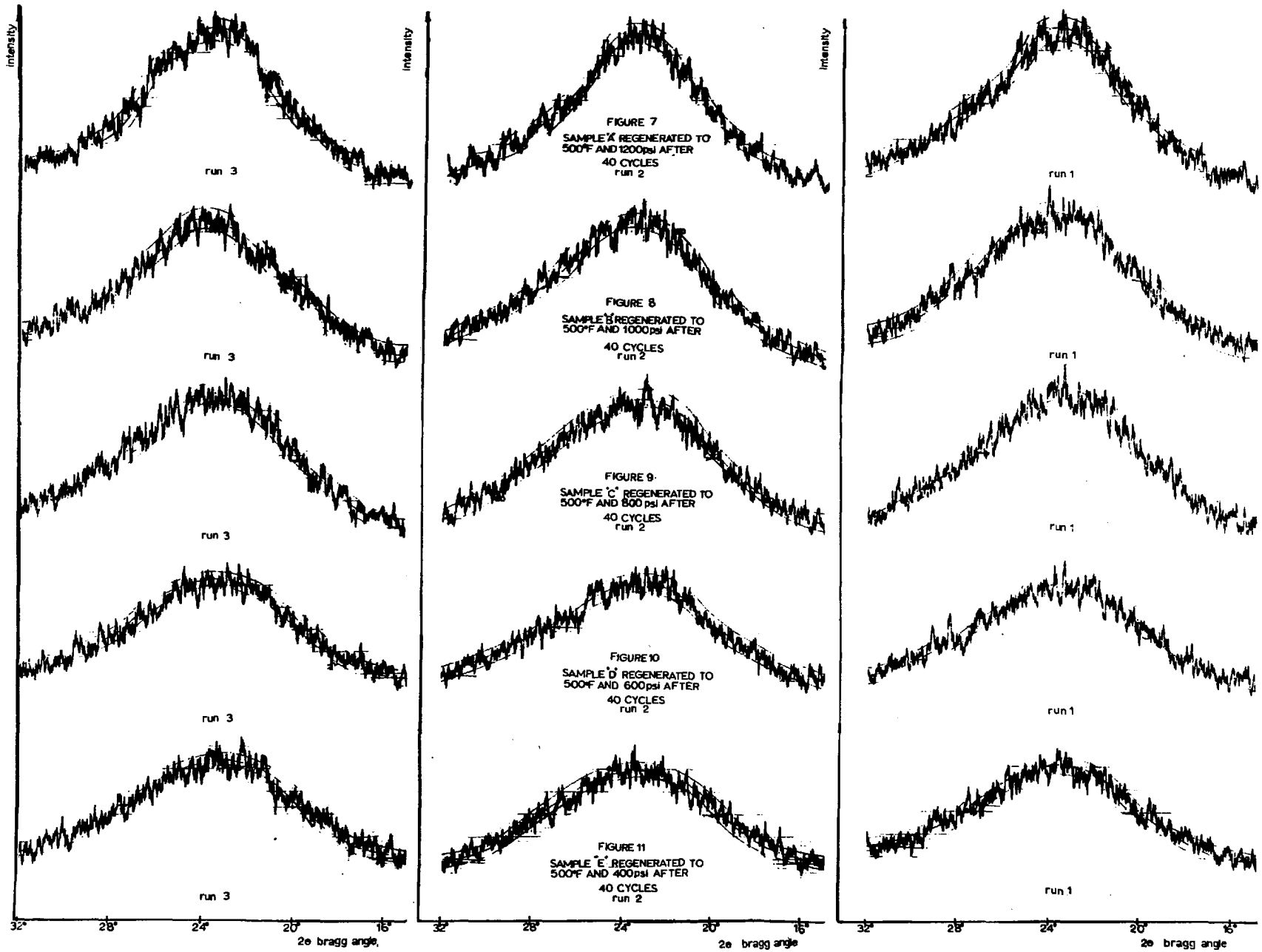

EFFECT OF TEMPERATURE ON SILICA GEL DIFFRACTION PATTERNS

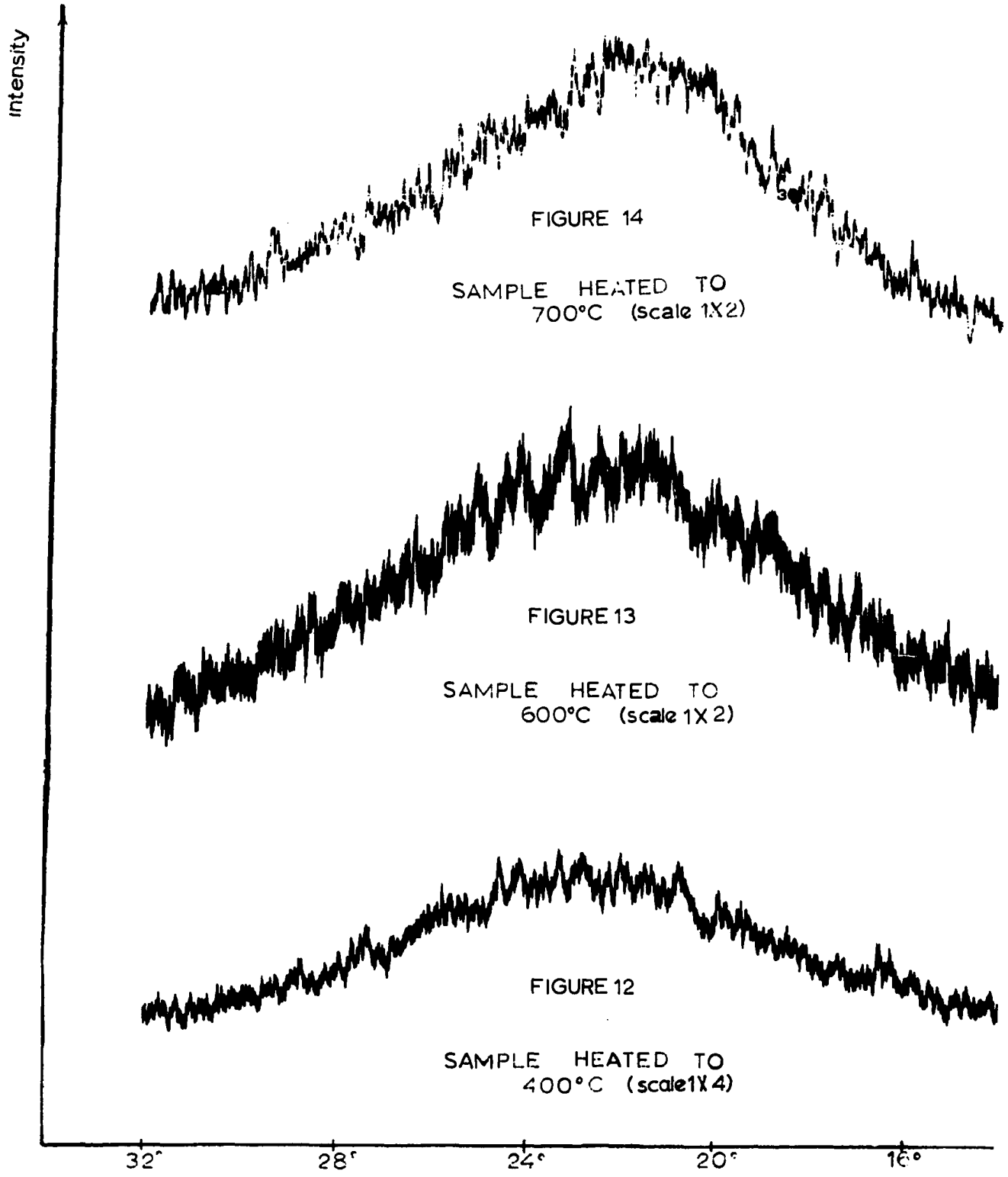

EFFECT OF TEMPERATURE ON SILICA GEL DIFFRACTION PATTERNS

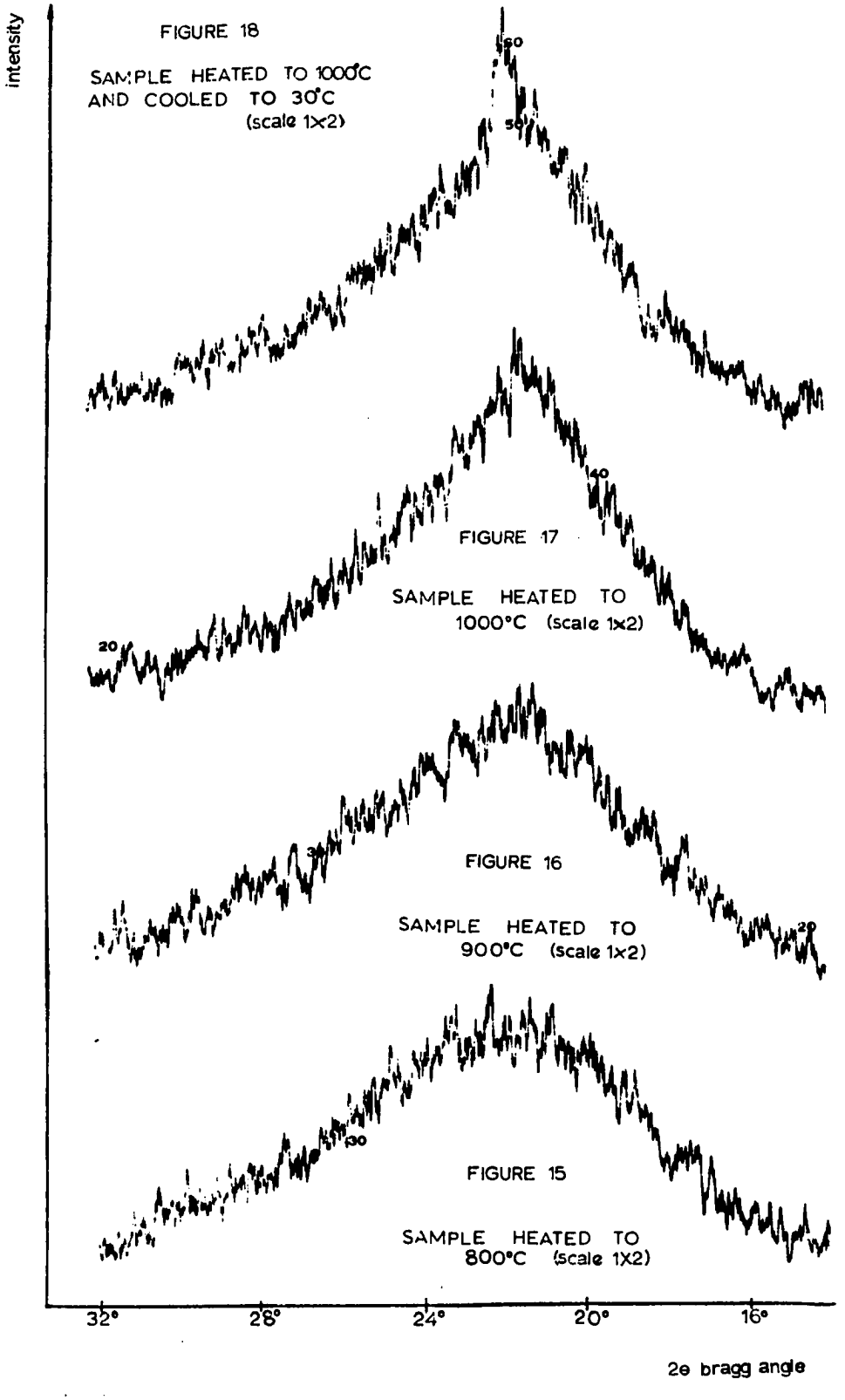

and atmospheric pressure. It is noted that this pattern shows a higher gain in crystallinity. The value of (W) seems to decrease considerably and the broad hollow shape which appeared at lower regeneration temperature is now a sharp steep pattern. This proves that silica gel can stand up to very high temperature under atmospheric pressure without gaining much crystallinity. On the other hand, the process of heating to a very high temperature (Figure 18) and cooling the gel to room temperature, causes the gel to change gradually from an amorphous substance to a partly crystalline one.

The above x-ray diffraction results, which show the relative effect of pressure and temperature on change in crystallinity, would all tend to produce a lower capacity. Although the relative change in crystallinity is pronounced, it is doubtful whether the absolute amount of crystallinity is sufficient to cause the degradation in capacity noted. This is not to say that development of crystallinity would not be a significant factor during the commercial life of silica gel which could easily involve as much as 20,000 cycles. Rather, it is recognition of the fact that gel fatigue, closing of pores, etc., are other possible factors that have not been investigated which could play a role. Regardless of the reasons, the proven loss of capacity is what is significant.

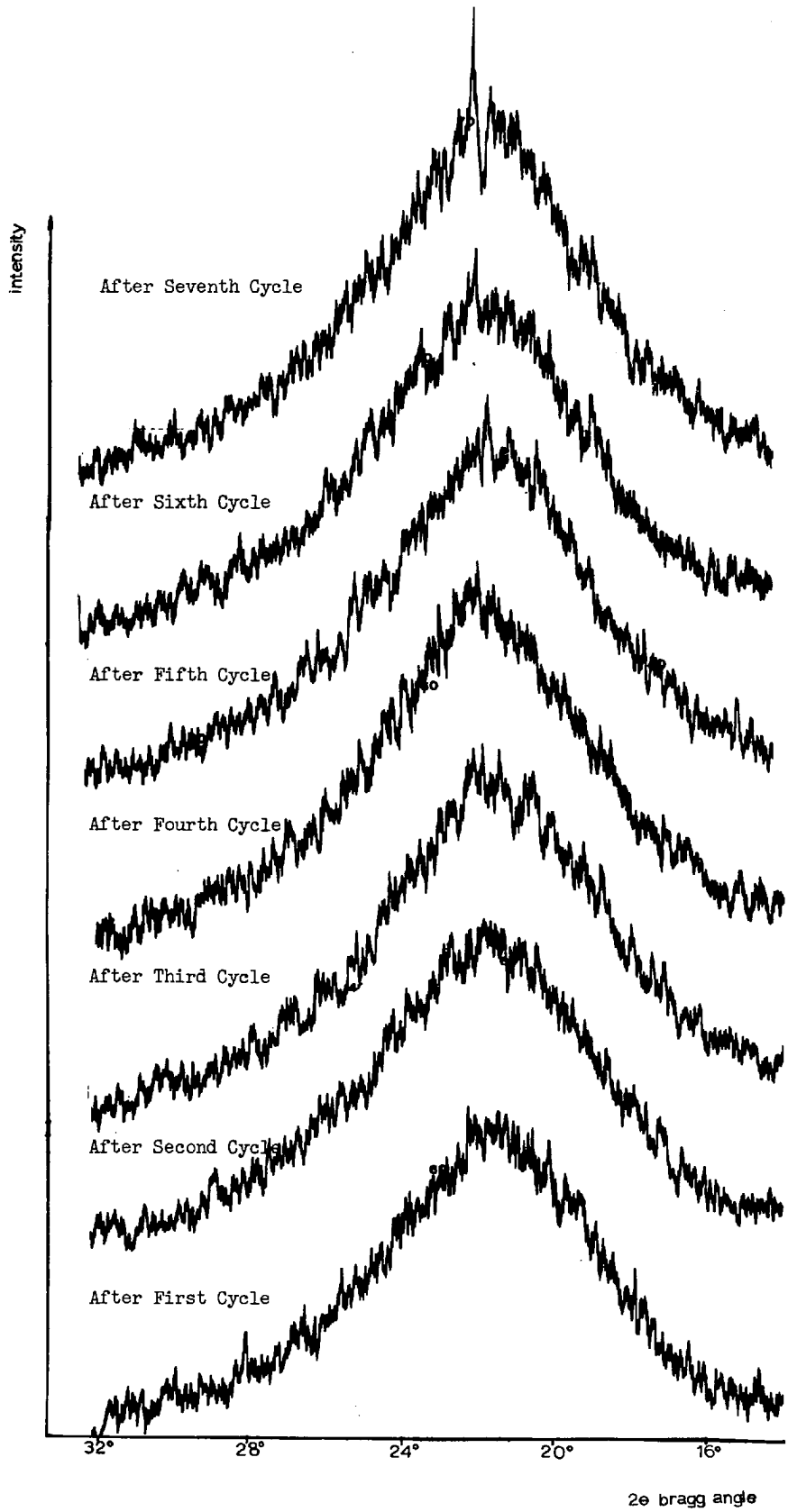
Intensity
After Seventh Cycle
After Sixth Cycle
After Fifth Cycle
After Fourth Cycle
After Third Cycle
After Second Cycle
After First Cycle
32°
28°
24°
20°
16°
2θ bragg angle

FIGURE 19

CHAPTER VI

CONCLUSIONS

This pioneer study has shown for the first time that exposure of amorphous silica gel to elevated pressures and temperatures for relatively short periods of time causes rapid changes in its characteristics. Specifically, it has been noted that:

1. The decrease in surface area and pore volume has been accompanied by a corresponding decrease in capacity for normal pentane.
2. A corresponding change in the character of the x-ray diffraction patterns occurs. These patterns show a change from high to low order diffraction patterns, i.e., a gradual increase in crystallinity is occurring.
3. For a given exposure time, loss in capacity increases with increased regeneration pressure at constant temperature.
4. Heating silica gel to a high temperature (above 900°C) at atmospheric pressure and then cooling it to room temperature increases crystallinity faster than continued high heating (below 900°C).
5. As regeneration pressure increases, the average "d" spacing

of the patterns decreases due to an increase in the Bragg angle and an increase of particle density.

6. An increase in the relative intensity (I/I_o) of silica gel is accompanied by a decrease in the surface area (S.A.) and the adsorptive capacity (X_T) of silica gel.

Based on these observations and data correlations presented, it has been possible to develop a semi-quantitative understanding of the interrelationships among the variables investigated. A basis is provided for future investigators to explore this area in greater depth.

BIBLIOGRAPHY

1. Andall, J. T. The Diffraction of X-Rays and Electrons by Amorphous Solids, Liquids and Gases, Chapman and Hall, New York (1934).

2. Ashford, F. E. M.P.E. Thesis, University of Oklahoma, (1963).

3. Bastick, J. Bull. Soc. Chim. France, 20, 437-44D (1953).

4. Boyd, G. E., Adamson, A. W., and Myers, L. S. J. Am. Chem. Soc. 69, 2836 (1947).

5. Brunauer, S. The Adsorption of Gases and Vapors, Princeton University Press, (1945).

6. Brunauer, S., Emmett, P. and Teller, L. J. Am. Chem. Soc. 60, 309 (1938).

7. Bunn, C. W. Chemical Crystallography, Oxford, Clarenton Press, London (1945).

8. Campbell, J. M. and Laurence, L. L. "Dehydration of Natural Gas and High Hydrocarbon Liquids," Petroleum Refiner, Volumes 31 and 32.

9. Campbell, J. M., Ashford, F. E., Needham, R. B., and Reid, L. S. "Design of Dynamic Hydrocarbon Adsorption Processes Employing Silica Gel," Petroleum Refiner, December (1963).

10. Campbell, J. M. "Review of Theoretical Development of Hydro-Carbon Recovery by Adsorption," Pamphlet presented to Davison Chemical Co., April (1962).

11. Carter, J. W. "Adsorption Processes," British Chemical Engineering 6, 308 (1961).

12. Cullity, B. D. Elements of X-Ray Diffraction, Addison-Wesley Publishing Co., Inc. (1959).

13. Dale, G. H. and Haskell, D. M. Chem. Engr. Progr. 57, 42 (1961).

14. Dow, W. M. Petroleum Refiner (April, 1957) 36 No. 4, pp. 141; and Oil and Gas Journal (Nov. 3, 1958) 56, 74.

14a. Frondel, Clifford. "The system of mkneralogy" (1962).

15. Gamson, B. W., Thodos, G. and Hougen, O. A. Trans. AIChE 1, 39 (1943).

16. Haley, A. J. "An Extension of the Nelsen-Eggersten Continuous Flow Method of Surface Area Measurements," Reprinted from J. of Appl. Chem. September 13 (1963).

17. Hougen, O. A. and Marshall, W. R. Chem. Eng. Prog. 43, 197 (1947).

18. Innes, W. B. Analytical Chemistry, 28, 332, (1956).

19. Jury, S. H. and Licht, W. Chem. Eng. Prog., February (1952) 102.

20. Klotz, I. M. "The Adsorption Wave," J. of Appl. Chem., April 3, (1946).

21. Klug, H. P. and Alexander, E. L. X-Ray Diffraction Procedures, John Wiley and Sons, Inc., (1954).

22. Koble, R. A. and Corrigan, T. E. Ind. Eng. Chem. 44, 383 (1952).

23. Krejci and Ott, E. J. Phys. Chem. 35, 2061-2064 (1931).

24. Ku, C. C., Huntington, R. L. and Reid, L. S. "Trans. AIME, 155, 253 (1944).

25. Leland, T. W. and Holmes, R. E. "The Design of Hydrocarbon Recovery Units Using Solid Adsorbents," J. of Petroleum Technology, 14, 179 (1962).

26. Mantell, C. E. Adsorption, New York, McGraw-Hill, (1951).

27. Marks, D. E., Robinson, R. J., Arnold C. W., and Hoffman, A. E. "Dynamic Behavior of Fixed-Bed Adsorbers," AIME, Paper No. 398, (1962).

28. Michaels, A. "Simplified Method of Interpreting Kinetic Data in Fixed Bed Ion Exchange," Industrial and Engineering Chemistry, Vol. 44, No 8, August (1952).

29. Milligan, W. O., and Hachford, H. H. J. Phys. and Colloid Chem. 51, 333 (1947).

30. Milliken, T. H., Mills, G. A. and Oblad, A. G. Discussions Faraday Soc. No 8, Hetrogeneous Catalysis, p. 279 (1950).

31. Nachod, F. C. Ion Exchange: Theory and Application, Academic Press Inc., New York, (1949).

32. Nash, D. B. "X-Ray Diffraction Studies on Silicate Rock Glasses," Jet Propulsion Laboratory Space Program Summary, No 37-20, 4:192, April 4, (1963).

33. Needham, R. B., Campbell, J. M. and McLeod, H. A. "A Critical Evaluation of the Mathematical Models Used for Dynamic Adsorption of Hydrocarbons," Unpublished article.

34. Parick, W. A., Froyer, J. C. and Rush, R. I. J. Phys. Chem. 31, 1511 (1927).

35. Ralph, K. I. The Colloid Chemistry of Silica and Silicates, Cornell University Press, Ithaca, New York (1955).

36. Randall, J. T., Rookby, H. P. and Cooper, B. S. The Diffraction of X-Rays by Vitreous Sclids and Its Bearing on Their Constitution, John Wiley and Sons, Inc., New York, (1934).

37. Ries, H. E. "Advances in Catalysis and Related Subjects," New York Academic Press, IV, 87, (1950).

38. Rosen, J. R. IEC August (1954).

39. Russell, A. S. and Cochran, N. C. "Alumina Surface Areas Measurements," Adsorption Symposiun, Reprinted from Ind. and Engr. Chemistry, Vol. 42, pp. 1279-1340.

40. Treybal, R. E. Mass Transfer Operations, McGraw-Hill Book Co., Inc., (1955).

41. Van Nordstrand, R. A., Kreger, W. E. and Ries, H. W. J. Phys. and Coll. Chem. 55, 541 (1951).

42. Vermuelen, T. Advanced in Chem. Engr. Vol. II, Academic Press, New York, (1958).

43. Walter, J. E. J. Chem. Phys. 13, 229 (1945).

44. Warren, B. E. "The Diffraction of X-Rays," Phys. Rev. 45, 657, (1934).

45. Weiser, H. B. Colloid Chemistry, J. Wiley, New York, (1949).

46. Wicke, E. "Untersuchungen uber Ad-und Desortpionsvorgange in kornigen, Durchstromten Adsorberschichten." Kolloic-Zeistchrift, 86, 167, 295 (1939).

APPENDIX A

APPENDIX A

TABLE 1

T.T.= 14.0

Regeneration Pressure 1200 psi

Sample A

03 GEL

3" tower (east)

wt. of gel = 17.58 lbs.

= 7,981 grms.

Time (Min)		C_5	C/C_o
t	t_a		
18	4	2.0	0.048
21	7	7.1	0.172
24	10	16.5	0.399
27	13	25.5	0.617
30	16	31.3	0.758
33	19	35.3	0.856
36	22	37.5	0.908
39	25	39.0	0.944
42	28	40.0	0.968
45	31	40.6	0.983
48	34	41.3	1.000
51	37	41.3	1.000

$C_o = 41.3$

$T\ (av) = 60.4^{\circ}F$
$T_B(av) = 93.3^{\circ}F$
$P_B(av) = 800.0$ psi
$P_w(av) = 18.05$ inches
$P\ (av) = 105.0$ psi
I.R. = 42.3 $\frac{grms}{min}$

$$Q = 36.27 \times 1.24 \times 1.0 \times \sqrt{18.05 \times 210}$$

$$= 44.97 \sqrt{3790}$$

$$= 44.97 \times 61.57$$

$$= 276\ SCF/HR$$

$$V = \frac{0.0102 \times 1769 \times 553.3}{815}$$

$$= 19.2\ ft/min$$

$$\text{mole } \% = \frac{42.3 \times 50.1}{72 \times 276} \times 100$$

$$= 1.06\%$$

TABLE 2

T.T. = 13.0

Regeneration Pressure 1000 psi

Sample B

03 GEL

3" tower (east

wt. of gel = 17.62 lbs

= 7,999 grms

Time (Min)			
t	t_a	C_5	C/C_o
18	5	2.1	0.048
21	8	7.6	0.174
24	11	16.8	0.383
27	14	24.9	0.568
30	17	31.3	0.713
33	20	35.4	0.806
36	23	38.5	0.875
39	26	39.9	0.908
42	29	41.0	0.935
45	32	42.4	0.965
48	35	43.6	0.993
51	38	43.8	0.997
54	41	43.9	1.000

$C_o = 43.9$

T (av) = 60.13°F
T_2 (av) = 91.08°F
P (av) = 800.0 psi
P_w (av) = 6.96 inches
P (av) = 105.0 psi
I.R. = 42.68 $\frac{\text{grms}}{\text{min}}$

$Q = 72.49 \times 1.0 \times \sqrt{6.96 \times 210}$
$= 72.49 \sqrt{1462}$
$= 72.49 \times 38.24$
$= 2.772$ SCF/HR

$$V = \frac{0.0102 \times 2722 \times 551.08}{815}$$

$= 19.2$ ft/min

$$\text{mole \%} = \frac{42.68 \times 50.1}{72 \times 2772} \times 100$$

$= 1.07\%$

TABLE 3

T.T. = 19.0

Regeneration Pressure 800 psi

Sample C

03 GEL

3" tower (east

wt. of gel = 17.61 lbs

= 7,995 grms

Time (Min)		C_5	C/C_o
t	t_a		
24	5	1.1	0.025
27	8	4.3	0.100
30	11	12.5	0.292
33	14	22.0	0.515
36	17	28.9	0.675
39	20	33.6	0.785
42	23	36.4	0.851
45	26	37.8	0.883
48	29	39.4	0.921
51	32	40.6	0.949
54	35	41.8	0.975
57	38	42.6	0.995
60	41	42.8	1.000

$C_o = 42.8$

T (av) = 60.0°F
T (av) = 92.0°F
P (av) = 800.0 psi
P^w (av) = 695 inches
P (av) = 105.0 psi
I.R. = 42.54 grms/min

$Q = 72.49 \times 1.0 \times \sqrt{6.95 \times 210}$

$= 72.49 \sqrt{1460}$

$= 72.49 \times 38.21$

= 2,770 SCF/HR

$$V = \frac{0.0102 \times 2770 \times 552}{815}$$

= 19.1 ft/min

$$\text{mole \%} \frac{42.54 \times 50.1}{72 \times 1770} \times 100$$

= 1.07 %

TABLE 4

T.T. = 9.0

Regeneration Pressure 600 psi

Sample D

03 GEL

3" tower (east)

wt. of gel = 17.83 lbs

= 8095 grms

Time (Min)		C_5	C/C_o
t	t_a		
14	5	0.5	0.013
17	8	2.9	0.070
20	11	9.8	0.232
23	14	20.3	0.481
26	17	26.6	0.633
29	20	30.9	0.735
32	23	34.1	0.811
35	26	35.8	0.850
38	29	37.4	0.888
41	32	39.2	0.930
44	35	40.2	0.955
47	38	41.6	0.988
50	41	42.0	0.998
53	44	42.1	1.000

C_o = 42.1

T (av) = 64.8°F
T (av) = 94.2°F
P (av) = 804.0 psi
(av) = 7.0 inches
P^W (av) = 105.0 psi

I.R. = 42.47 grms/min

$Q = 72.49 \times 0.9954 \sqrt{7.0 \times 210}$
$= 72.16 \sqrt{1470}$
$= 72.16 \times 38.35$
$= 2767$ SCF/HR

$$V = \frac{0.0102 \times 2767 \times 554.2}{815}$$

= 19.1 ft/min

$$\text{mole \%} = \frac{42.47 \times 50.1}{72 \times 2767} \times 100$$

= 1.06%

TABLE 5

T.T. = 10.0

Regeneration Pressure 400 psi

Sample E

03 GEL

3" tower (east)

wt. of gel = 17.68 lbs

= 8,207 grms

Time (Min) t	t_a	C_5	C/C_o
15	5	0.4	0.010
18	8	2.0	0.045
21	11	8.7	0.201
24	14	20.0	0.460
27	17	26.6	0.611
30	20	31.4	0.721
33	23	34.6	0.795
36	26	26.4	0.837
39	29	38.4	0.882
42	32	39.8	0.915
45	35	41.2	0.946
48	38	42.4	0.974
51	41	43.1	0.991
54	44	43.5	1.000

C_o = 43.5

$T_{(av)}$ = 63.6°F
$T_{(av)}$ = 92.8°F
$P_{(av)}$ = 800.0 psi
$P^w_{(av)}$ = 7.0 inches
$P_{(av)}$ = 105.0 psi
I.R. - 41.86 grms/min

$Q = 72.49 \times 0.9966 \times \sqrt{7.0 \times 210}$
$= 72.24 \sqrt{1470}$
$= 72.24 \times 38.35$
$= 2.770$ SCF/HR

$$V = \frac{0.0102 \times 2770 \times 552.8}{8.5}$$

= 19.2 ft/min

$$\text{mole \%} = \frac{41.86 \times 50.1}{72 \times 2770} \times 100$$

= 1.05%

TABLE 6

T.T. = 10.0

Regeneration Pressure 800 psi (80 cycles)

Sample F

03GEL

3" tower (east)

wt. of gel = 17.73 lbs

= 8,049 grms

Time (Min)		C_5	C/C_o
t	t_a		
15	5	0.2	0.038
18	8	6.2	0.152
21	11	13.5	0.331
24	14	21.1	0.517
27	17	28.3	0.692
30	20	32.5	0.794
33	23	35.3	0.863
36	26	36.5	0.893
39	29	38.0	0.929
42	32	39.2	0.959
45	35	41.0	0.981
48	38	40.5	0.990
51	41	40.9	1.000

$C_o = 40.9$

$T_{(av)} = 65.66^{\circ}F$

$T_{(av)} = 91.38^{\circ}F$

$P_{(av)} = 800.0$ psi

$w_{(av)} = 7.0$ inches

$P_{(av)} = 105$ psi

I.R. = 42.04 grms/min

$Q = 72.49 \times 0.9946 \times \sqrt{7.0 \times 210}$

$= 72.900 \sqrt{1470}$

$= 72.099 \times 38.35$

$= 2{,}765$ SCF/HR

$$V = \frac{0.102 \times 2765 \times 551.38}{815}$$

$= 19.1$ ft/min

$$\text{mole } \% = \frac{42.04 \times 50.1}{72 \times 2765} \times 100$$

$= 1.06\%$

TABLE 6(a)

T.T. = 12.0

Fresh Sample (not subject to regeneration)

Sample E'

03 GEL

3" tower (east)

wt. of gel = 17.62 lbs

= 7,999 grms

Time (Min)		C_5	C/C_o
t	t_a		
18	6	0.3	0.007
21	9	1.7	0.039
24	12	8.0	0.185
25	15	18.2	0.419
30	28	25.0	0.574
33	21	30.1	0.692
36	24	33.4	0.765
39	27	35.2	0.811
42	30	38.0	0.872
45	33	39.0	0.900
48	36	41.0	0.940
51	39	41.9	0.962
54	42	42.4	0.975
57	45	43.0	0.992
60	48	43.5	1.000

T_f (av) = 63.0°F
T_B^f (av) = 93.1°F
P_B(av) = 800.0 psi
^{w} (av) = 7.0 inches
P_f (av) = 105.0 psi
I.R. = 42.01 grms/min

$$Q = 72.49 \times 1.0 \times \sqrt{7.02 \times 210}$$
$$= 72.49 \sqrt{1470}$$
$$= 72.49 \times 38.35$$
$$= 2{,}779 \text{ SCF/HR}$$

$$\bar{V} = \frac{0.0102 \times 2779 \times 553.1}{815}$$

$$= 19.25 \text{ ft/min}$$

$$\text{Mole \%} = \frac{42.01 \times 50.1}{72 \times 2779} \times 100$$

$$= 1.052\%$$

TABLE 7

SUMMARY OF ADSORPTION RESULTS

Code	Run	Gel	Ads. Press.	Inlet Temp.	Flow G	Rate V	Bed Length	Bed Dens	Mole Percent	Inj. Rate	Reg. Pressure
3311	A	101	800	93.3	3003	19.31	210.2	.891	1.0629	42.30	1200
3311	B	101	800	91.2	3007	19.26	210.9	0.890	1.0713	42.6	1000
3311	C	101	800	92.0	3005	19.28	209.0	.898	1.0686	42.54	800
3311	D	101	800	94.2	3001	19.33	216.9	.876	1.0629	41.27	600
3311	E	101	800	92.8	3005	19.30	211.5	.891	1.0515	41.86	400
3311	E'	101	800	93.1	3006	19.25	211.0	.890	1.0532	42.01	0
3311	F	101	800	91.4	2999	19.22	211.1	.958	1.0579	42.04	200

N: E' = run on a fresh gel.

Run	Time E	Time B	Time F	F	QZ	Bed Wt.	X_T	X_B	V_Z	Reg. Cycles
A	26.0	4.7	13.36	.371	333	17.57	.0669	.0251	16.62	40
B	30.2	5.1	15.79	.371	398	17.61	.0771	.0273	14.58	40
C	32.0	6.4	16.40	.358	390	17.61	.0833	.0344	13.34	40
D	34.2	7.1	17.41	.357	410	17.83	.0879	.0372	12.88	40
E	35.2	7.8	17.87	.346	396	17.68	.0905	.0411	12.17	40
F	35.1	8.2	18.02	.330	374	17.62	.0908	.0451	11.51	0
G	51.2	5.6	16.11	.371	400	17.72	.0790	.0293	11.39	80

TABLE 8

Sample	Pressure psi	Surface Area m^2/grm	Pore Volume cc/grm	Particle Density grm/cc
A	1200	561	0.31	1.34
B	1000	684	0.38	1.23
C	800	668	0.39	1.21
D	600	691	0.40	1.19
E	400	727	0.42	1.17
*F	800	658	0.38	1.23

*Sample regenerated for 80 cycles.

TABLE 9

Sample	Pressure psi	Peak Height Inches	Relative Intensity I/I_o
A	1200	3.38	1.000
B	1000	2.90	0.858
C	800	2.86	0.846
D	600	2.17	0.642
E	400	2.05	0.607
E'	0	1.91	0.562

*E' = fresh sample of gel.

TABLE 10

Sample	Pressure psi	Area Under Pattern in^2	Relative Area Under Pattern A/A_o
A	1200	13.4	1.000
B	1000	11.8	0.891
C	800	11.6	0.866
D	600	9.2	0.687
E	400	8.5	0.634

TABLE 11

Sample	Pressure psi	Width of Patterns At Half Maximum Height in	Relative Width W/W_o
A	1200	3.35	0.835
B	1000	3.70	0.923
C	800	3.89	0.970
D	600	3.96	0.988
E	400	4.01	1.000